NATIONAL ADVISORY COMMITTEE FOR AERONAUTICS

TECHNICAL NOTE 2317

APPLICATIONS OF VON KÁRMÁN'S INTEGRAL METHOD IN SUPERSONIC WING THEORY

By Chieh-Chien Chang

The Johns Hopkins University

Washington
March 1951

NATIONAL ADVISORY COMMITTEE FOR AERONAUTICS

TECHNICAL NOTE 2317

APPLICATIONS OF VON KÁRMÁN'S INTEGRAL METHOD IN SUPERSONIC WING THEORY

By Chieh-Chien Chang

SUMMARY

The present paper derives Von Kármán's Fourier integral method in supersonic wing theory directly from the basic concepts of the harmonic source and doublet. The method is first applied to investigate the general solution of the wave drag of a tapered swept wing with a symmetrical diamond airfoil profile. The general solution includes all kinds of wing plan forms which may be swept backward or forward, and tapered or reversely tapered to any ratio. A number of the limiting cases are also investigated. For practical aerodynamic design, two families of wing plan forms with the fixed taper ratios 0.2 and 0.5, any swept angle, aspect ratio, and Mach number are shown in graphs. Some particular applications are illustrated.

The reversed-flow theorem on wave drag as shown by Von Kármán and Hayes checks well with the consequence of the general solution. This method shows a certain elegance as no conical-flow assumption is needed and the mathematics is powerful enough to obtain a general solution covering all possible geometrical arrangements without detailed considerations.

While in recent years the direct problem of finding the lift distribution with a given angle of attack of the wing has been well solved by the method of conical flow and by other methods, the present treatment, on the other hand, investigates the inverse problem, that is, to find the downwash distribution in the plane of a wing with a preassigned pressure distribution. This is particularly favorable with the present method. The general solution of the downwash of the tapered swept wings is derived for the case where a constant lift distribution on the wing is preassigned. Of course, the method may be applied to any lift or pressure distribution along the wing chord and span. The corresponding angle of attack of the wing and the downwash can be determined everywhere in the plane of the wing. To demonstrate the downwash distribution as given by the general solution, the downwash of a number of wings, including a sweptback tapered wing with supersonic trailing edge and a triangular wing, is shown in graphs.

The general solution of the direct problem in the present formulation is a singular integral equation of the Weiner-Hopf type and is difficult to obtain.

INTRODUCTION

In 1935 Von Kármán first showed that the concept of the Fourier integral can be adopted to explain the similarity of Prandtl wing theory and the theory of planing surfaces (reference 1). In 1946, Von Kármán introduced the Fourier integral method to the supersonic wing theory (an unpublished report of Northrop Aircraft, Inc.). The present author under Von Kármán's guidance investigated this problem to a certain extent; some of the results have been published (reference 2) but some, presented in 1948 at the Sixth International Congress for Applied Mechanics, are not available in published form. The present report may be considered as an extension of the earlier work. As some of the literature is unavailable at this moment, some of Von Kármán's work is repeated.

As far as the linearized theory on supersonic wings is concerned, the conical-flow method was originated by Busemann (reference 3) and later reproduced and extended by Lagerstrom (reference 4), Hayes (reference 5), Stewart (reference 6), Laporte and Bartels (reference 7), and Snow (reference 8). Each of the later investigators approached the same method with slightly different techniques but confirmed the essential results of Busemann. Before the conical-flow method was known in this country, Jones visualized the advantages of the conical flow and showed some of the basic physical concepts (reference 9) in 1945. Later, in 1946, with the concept of conical flow, Jones also showed the invariance of the Lorentz transformation and introduced the oblique coordinate in the swept-wing problem (reference 10).

The challenge of supersonic flight has aroused the interest of many other investigators. Puckett showed that the source integration method could be applied to study the wave drag problem (reference 11). Later Evvard extended this method to solve the lift problem of a finite wing of any plan form (references 12 and 13). Heaslet, Lomax, and Jones extended Volterra's and Hadamard's method to the supersonic wing problem (references 14 and 15). Gunn applied the operational calculus to the same problem (reference 16). There are many other works, all of which cannot be mentioned in this paper.

On the other hand, the basic concept of the Fourier integral method is quite different from the above methods. Instead of the concept of conical flow or simple sources and doublets, the present method considers along the direction of flight infinitely long harmonic source (or doublet)

lines, the behavior of which is quite equivalent to the harmonic acoustic source (or doublet) in the sequence of time. Each of such source lines will send out a divergent cylindrical wave in the radial direction. The potential of such a wave can be expressed by the product of the source-strength function and the Hankel function of the second kind. For each eigenvalue or frequency of the source oscillation, there is a corresponding eigenvalue in the argument of the Hankel function. By means of the principle of superposition, an arbitrary distribution can be synthesized with such simple harmonic sources of different frequencies, if the frequency spectrum is a continuous one. The most powerful technique to serve such a purpose is the Fourier integral method.

Now in the finite-wing problem, the boundary is considered as a source sheet rather than as source lines. Such a sheet can be built up by integrating elements of a source strip which is equivalent to a source line in behavior.

The above simple physical interpretation may help to give some insight into the mathematical theory to be discussed later.

The present paper first tries to give an introduction to Von Kármán's method in terms of the physical rather than mathematical approach. Then, the wave drag of a tapered sweptback wing is treated. This work is not a duplication of that of some other concurrent investigators, but rather a supplementary contribution. The next step is the lift problem. For a given angle of attack, on an arbitrary wing plan form, it is rather difficult to solve the integral equation analytically. But for a given lift distribution the downwash angle can be evaluated anywhere in the plane of the wing.[1]

The method has a certain elegance. The complete physical effect of the arbitrary wing can be expressed in terms of one integral. The finite number of discontinuous points of the Fourier-Bessel integral gives exactly the right picture.

This investigation was conducted at the Department of Aeronautics of the Johns Hopkins University under the sponsorship and with the financial assistance of the National Advisory Committee for Aeronautics. Due appreciation should be given to Misses V. O'Brien and P. Clarken for their assistance in carrying out the research.

---

[1]In some recent unpublished Navy reports, J. D. Miles has obtained a solution of the direct problem, particularly for the rectangular wing tip with constant angle of attack.

GENERAL THEORY OF THE FOURIER INTEGRAL METHOD

Elementary Solutions

In the three-dimensional, steady supersonic flow of a compressible nonviscous fluid, the differential equation of motion in the linearized sense is

$$\phi_{yy} + \phi_{zz} = \left(M^2 - 1\right)\phi_{xx} \tag{1}$$

where the velocity potential ϕ is defined by grad $\phi = \bar{q} - U\bar{i} = u\bar{i} + v\bar{j} + w\bar{k}$, the disturbance velocity vector. It may be considered as a two-dimensional wave equation if x is conceived as time in the sequence of which the future can contribute nothing to the present. This can be shown clearly by introducing $t = \dfrac{x}{\left(M^2 - 1\right)^{1/2}}$; that is,

$$\phi_{yy} + \phi_{zz} = \phi_{tt} \tag{2}$$

with the dimension in the flow direction being equivalent to time t. After this transformation, the velocity of propagation in equation (2) is unity. In this sense, equation (2) becomes the potential problem of the acoustic source and doublet in the y,z-plane in the sequence of time as pointed out by Von Kármán (reference 2). After this transformation, the wing plan form has to be readjusted so that the Mach waves are inclined backward at 45° from the flow direction. As an example of transformation, figure 1 gives a sweptback wing in the physical and transformed planes.

For a simple time-dependent harmonic source with strength $\cos \lambda t$ (where $\lambda/2\pi$ is the frequency of oscillation) located at $(\eta,0)$ in the y,z-plane, the elementary solution of equation (1) as given by Lamb (reference 17, p. 297) is

$$\phi_o(t,y,z;\ \eta,0) = \mathrm{Re}\left[-\frac{i}{4} e^{i\lambda t} H_0^{(2)}(\lambda r)\right] \tag{3}$$

where $r = \sqrt{(y - \eta)^2 + z^2}$ and $H_0^{(2)}(\lambda r)$ is the Hankel function of the second kind of zero order. It is easy to show that the solution satisfies

both the differential equation (2) and the given boundary condition $\cos \lambda t = \text{Re } e^{i\lambda t}$. At very large values of λr equation (3) becomes

$$\phi_o(t,r) \approx \frac{1}{\sqrt{8\pi\lambda r}} \cos\left[\lambda(t - r) - \frac{\pi}{4}\right]$$

the amplitude of which is inversely proportional to the square root of r. Physically, this represents the potential at the point (y,z) at time t due to a harmonic source of strength $\cos \lambda t$ at distance r from it. Such a disturbance potential is called a divergent wave. This disturbance propagates from the point $(\eta,0)$ with a circular or cylindrical symmetry.

Now if the strength of the source is the real part of $F(\lambda)e^{i\lambda t}$ instead of just $e^{i\lambda t}$, the potential must be also written as

$$\phi_o(t,y,z;\ \eta,0) = \text{Re}\left[-\frac{i}{4} F(\lambda)e^{i\lambda t} H_o^{(2)}(\lambda r)\right] \tag{4}$$

where

$$F(\lambda) = F_0(\lambda) + iF_1(\lambda) \tag{5}$$

with $F_0(-\lambda) = F_0(\lambda)$ being even and $F_1(-\lambda) = -F_1(\lambda)$ being odd. It is understood that $F(\lambda)$ is a function representing the strength, amplitude, and location of the source line.

If two such harmonic line sources of equal but opposite strength - the negative one located at $(\eta,-\zeta/2)$ and the positive one at $(\eta,\zeta/2)$ - approach each other, a harmonic doublet line can be obtained if $\lim_{\zeta \to 0} F(\lambda)\zeta = G(\lambda)$ is considered as a finite quantity:

$$\begin{aligned}
\phi_1(t,y,z;\ \eta,0) &= \lim_{\zeta \to 0}\left[\phi_o\left(t,y,z;\ \eta,\frac{\zeta}{2}\right) - \phi_o\left(t,y,z;\ \eta,\frac{-\zeta}{2}\right)\right] \\
&= \lim_{\zeta \to 0} \frac{\partial \phi_o}{\partial \zeta}\zeta \\
&= \text{Re}\left[-\frac{i\lambda}{4} G(\lambda)e^{i\lambda t} H_1^{(2)}(\lambda r)\frac{z}{r}\right]
\end{aligned} \tag{6}$$

where the doublet is defined as positive, and

$$G(\lambda) = G_0(\lambda) + iG_1(\lambda) \tag{7}$$

with $G_0(-\lambda) = G_0(\lambda)$ being even and $G_1(-\lambda) = -G_1(\lambda)$ being odd. It is very interesting to see that this potential of the doublet no longer has cylindrical symmetry, but is antisymmetrical with respect to the t,y-plane. The harmonic doublet line will be used for the wing lift problem.

Boundary Conditions in the Supersonic Wing Problem

Let a flat body or wing occupy a region in the x,y-plane and α_+ and α_- be the slopes of the upper and lower wing surfaces at (x,y), respectively. Both are small in comparison with unity and are zero outside the finite region occupied by the wing. Within the approximation of the linearized theory, the wing may be considered equivalent to the superposition of a symmetrical body and a mean-cambered surface. The slope of the symmetrical body is

$$\alpha_o = \frac{1}{2}(\alpha_+ - \alpha_-) \tag{8}$$

and the slope of the cambered surface is

$$\alpha_1 = \frac{1}{2}(\alpha_+ + \alpha_-) \tag{9}$$

where α_o and α_1 are considered at the x,y-plane. In other words, the effect of exact location of α_o and α_1 in the z-direction is entirely neglected in the future treatment which has been shown by Von Kármán to be consistent with the linearized theory for the flat body. From the above, the required boundary condition of the potential is the normal velocity to the wing surface which is zero; that is,

$$\bar{q}\bar{n} = 0 \tag{10}$$

In this case of a flat body, where the vertical velocity component predominates, equation (10) can be approximately expressed by

$$w_+ = \left(\frac{\partial \phi}{\partial z}\right)_{z=+0} = U\alpha_+ \tag{11}$$

$$w_- = \left(\frac{\partial \phi}{\partial z}\right)_{z=-0} = U\alpha_- \tag{12}$$

where w_+ and w_- represent vertical velocity components on the top and bottom of wing surfaces, respectively. Besides, at a distance far away from the wing in the upper stream, $u = v = w = 0$ if there is no other disturbance generated in the upper stream.

Supersonic Flow about a Flat Symmetrical Body

If a source line at $(\eta,0)$ is of any arbitrary strength with finite time t the potential can be built up with equation (4) by means of a Fourier integral as

$$\phi_o'(t,y,z) = \mathrm{Re} \int_{\to 0}^{\infty} d\lambda \left[-\frac{Ui}{4} F(\lambda,\eta) e^{i\lambda t} H_0^{(2)}(\lambda r) \right] \tag{13}$$

where U is the free-stream velocity. The insertion of U in the source-strength function is purely for future convenience.

The above integral and its first derivatives exist if the Lebesgue integral

$$\int_0^{\infty} \lambda \left| F(\lambda,\eta) H_0^{(2)}(\lambda r) \right| d\lambda < \infty$$

The above condition is automatically satisfied, if the source with finite strength is in action for a finite time interval. Actually, equation (13) can be considered as the potential of a body of revolution. Sometimes, in conforming with the convention of the complex Fourier integral, the above equation may be conveniently written as

$$\phi_o'(t,y,z) = -\frac{Ui}{8} \int_{-\infty}^{\infty} d\lambda F(\lambda,\eta) e^{i\lambda t} H_0^{(2)}(\lambda r) \tag{14}$$

with the understanding that the path of integration of λ is slightly above or below the origin in the complex λ-plane so that the singularity at $\lambda = 0$ can be detoured. It can be verified easily because

$$F(-\lambda,\eta) = F_0(\lambda,\eta) - iF_1(\lambda,\eta) = \overline{F(\lambda,\eta)}$$

$$H_0^{(2)}(-\lambda r) = H_0^{(2)}\left(\lambda re^{i\pi}\right) = H_0^{(2)}\left(\lambda re^{-i\pi}\right) = \overline{H_0^{(2)}(\lambda r)}$$

where the bar represents the complex conjugate of the original function. Now, the above source line may be considered as an elementary strip of a source sheet in the t,y-plane of width $d\eta$ with the above strength as the strength density per unit area. It is clear then that the potential due to a source sheet built up by such strips is

$$\phi_0(t,y,z) = \int_{-\infty}^{\infty} \phi_0' \, d\eta$$

$$= -\frac{Ui}{8} \int_{-\infty}^{\infty} d\eta \int_{-\infty}^{\infty} d\lambda F(\lambda,\eta) e^{i\lambda t} H_0^{(2)}(\lambda r) \qquad (15a)$$

For the convenience of the later development, $f(\lambda,\eta) = -\frac{1}{4} F(\lambda,\eta)$ is introduced into equation (15a), and then

$$\phi_0(t,y,z) = \frac{Ui}{2} \int_{-\infty}^{\infty} d\eta \int_{-\infty}^{\infty} d\lambda f(\lambda,\eta) e^{i\lambda t} H_0^{(2)}(\lambda r) \qquad (15b)$$

One thing should be pointed out. Owing to the structure of the integral, the source sheet may be composed of a number of discontinuous portions in the y-direction, and the source-strength function $f(\lambda,\eta)$ may be different in different discontinuous portions, but it must be the same within one continuous portion of the source sheet. Of course, in that case, the integration with respect to η has to be broken up accordingly. Physically, this integral can give the potential not only due to one wing but also to a number of wings or flat bodies in the t,y-plane. Therefore, it can be used to study the interaction between wings.

The preceding equation will be the disturbance potential of the wing, if the relation of the source-strength function $\mathrm{Re}\, f(\lambda,\eta)e^{i\lambda t}$ can be identified with α_o or the thickness distribution of the symmetrical flat body. This can be obtained from the boundary condition. Differentiating equation (15b) with respect to z, there results

$$\frac{\partial \phi_o}{\partial z} = -\frac{Ui}{2}\int_{-\infty}^{\infty} d\eta \int_{-\infty}^{\infty} \lambda\, d\lambda f(\lambda,\eta)e^{i\lambda t}H_1^{(2)}(\lambda r)\frac{z}{r} \tag{16}$$

Now as $z \longrightarrow 0$ the integrand goes to zero except in the neighborhood of $\eta = y$. Let $\eta = y + z \tan\theta$; $d\eta = z \sec^2\theta\, d\theta$, where $\theta = \tan^{-1}\frac{\eta - y}{z}$.

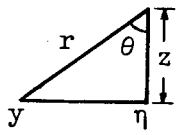

Besides, $H_1^{(2)}(\lambda r) \approx 2i/\pi\lambda r$ when λr or $r \longrightarrow 0$. Thus equation (16) becomes

$$(w)_{z=+0} = \left(\frac{\partial \phi_o}{\partial z}\right)_{z=+0}$$

$$= \lim_{z \longrightarrow +0} -\frac{Ui}{2}\int_{-\infty}^{\infty} d\lambda e^{i\lambda t}\int_{-\pi/2}^{\pi/2} \lambda f(\lambda, y + z\tan\theta)\,\frac{2i}{\pi\lambda}\,\frac{z^2}{r^2}\sec^2\theta\, d\theta$$

$$= \lim_{z \longrightarrow +0} \frac{U}{\pi}\int_{-\infty}^{\infty} d\lambda e^{i\lambda t}\int_{-\pi/2}^{\pi/2} \lambda f(\lambda, y + z\tan\theta)\, d\theta$$

$$= \frac{U}{\pi}\int_{-\infty}^{\infty} d\lambda e^{i\lambda t} f(\lambda,y)\int_{-\pi/2}^{\pi/2} d\theta$$

$$= U\int_{-\infty}^{\infty} d\lambda e^{i\lambda t} f(\lambda,y) \tag{17}$$

From equation (10),

$$(w)_{z=+0} = U(\alpha_o)_{z=+0} = U\int_{-\infty}^{\infty} d\lambda e^{i\lambda t} f(\lambda,y)$$

or

$$\alpha_o(t,y,+0) = \int_{-\infty}^{\infty} d\lambda e^{i\lambda t} f(\lambda,y)$$

$$= 2\int_{0}^{\infty} \left[f_0(\lambda,y)\cos \lambda t + f_1(\lambda,y)\sin \lambda t\right] d\lambda \qquad (18)$$

From the theory of complex Fourier transform,

$$f(\lambda,y) = \frac{1}{2\pi}\int_{-\infty}^{\infty} \alpha(t,y)e^{-i\lambda t}\, dt \qquad (19)$$

This means that, if the source distribution $f(\lambda,y)$ is chosen to be the Fourier transform of the distribution of the angle of attack, the potential ϕ_o will represent the flow about the wing automatically. Since the angle of attack is zero ahead of the wing, it can be shown easily that equation (15b) satisfies the second boundary condition of equation (12).

Supersonic Flow about a Lifting Surface

By means of the same argument as in the last section, the potential can be formulated for a doublet sheet of strength $\mathrm{Re}\, e^{i\lambda t}G(\lambda,\eta)$ from equation (6):

$$\phi_1(t,y,z) = \mathrm{Re}\,\frac{-iU}{4}\int_{-\infty}^{\infty} d\eta \int_{0}^{\infty} d\lambda\, \lambda\, G(\lambda,\eta)e^{i\lambda t}H_1^{(2)}(\lambda r)\frac{z}{r} \qquad (20)$$

where a constant, free-stream velocity U is introduced. In order to simplify the later development, further introduce

$$g(\lambda,\eta) = \frac{i\lambda G(\lambda,\eta)}{8m'} = g_0(\lambda,\eta) - ig_1(\lambda,\eta) \tag{21}$$

where, with equation (7),

$$\left.\begin{aligned} g_0(\lambda,\eta) &= \frac{\lambda G_1(\lambda,\eta)}{8m'} \qquad \text{(even)} \\ g_1(\lambda,\eta) &= \frac{\lambda G_0(\lambda,\eta)}{8m'} \qquad \text{(odd)} \end{aligned}\right\} \tag{22}$$

Then equation (20) can be written

$$\phi_1(t,y,z) = \mathrm{Re}\left[-2m'U \int_{-\infty}^{\infty} d\eta \int_0^{\infty} d\lambda g(\lambda,\eta) e^{i\lambda t} H_1^{(2)}(\lambda r)\frac{z}{r}\right] \tag{23}$$

The above equation can be written entirely in the complex form

$$\phi_1(t,y,z) = -m'U \int_{-\infty}^{\infty} d\eta \int_{-\infty}^{\infty} d\lambda g(\lambda,\eta) e^{i\lambda t} H_1^{(2)}(\lambda r)\frac{z}{r} \tag{24}$$

if the path of λ is chosen below $\lambda = 0$ in the complex λ-plane, because

$$\left.\begin{aligned} \overline{g(-\lambda,\eta)} &= g_0(\lambda,\eta) + ig_1(\lambda,\eta) = g(\lambda,\eta) \\ H_1^{(2)}(-\lambda r) &= H_1^{(2)}\left(\lambda r e^{-i\pi}\right) = \overline{H_1^{(2)}(\lambda r)} \end{aligned}\right\} \tag{25}$$

The path of λ with $\mathrm{Re}\ \lambda > 0$ cannot be chosen in order to detour $\lambda = 0$. In that case,

$$H_1^{(2)}(-\lambda r) = H_1^{(2)}\left(\lambda r e^{i\pi}\right) = -H_1^{(2)}(\lambda r) - 2J_1(\lambda r) \neq \overline{H_1^{(2)}(\lambda r)}$$

which is impossible to reduce back to the original equation (23).

In order to find out whether equation (24) for the doublet sheet satisfies all the boundary conditions of the wing or not, first differentiate it with respect to t.

$$\frac{\partial \phi_1}{\partial t} = m' \frac{\partial \phi_1}{\partial x} = m'u = -m'Ui \int_{-\infty}^{\infty} d\eta \int_{-\infty}^{\infty} \lambda \, d\lambda g(\lambda,\eta) e^{i\lambda t} H_1^{(2)}(\lambda r) \frac{z}{r} \qquad (26)$$

The above equation is identical in form with equation (16) if $f(\lambda,\eta)$ is replaced by $\frac{m'}{2} g(\lambda,\eta)$. Therefore, with the same technique, it can be shown that, as $z \longrightarrow +0$, $\eta \longrightarrow y$.

$$\left(\frac{\partial \phi_1}{\partial t}\right)_{z=+0} = \frac{-m'U}{2} \int_{-\infty}^{\infty} d\lambda e^{i\lambda t} g(\lambda,y) \qquad (27)$$

Now in the linearized theory the pressure coefficient on the wing surface is

$$C_p(t,y,+0) = \frac{-2u}{U} = \frac{-2}{Um'}\left(\frac{\partial \phi_1}{\partial t}\right)_{z=+0} \qquad (28)$$

Thus, with equation (27),

$$C_p(t,y,+0) = \int_{-\infty}^{\infty} d\lambda e^{i\lambda t} g(\lambda,y) \qquad (29)$$

With the Fourier transform,

$$g(\lambda,y) = \frac{1}{2\pi} \int_{-\infty}^{\infty} dt e^{i\lambda t} C_p(t,y,+0) \qquad (30)$$

Therefore, if the pressure distribution along the wing chord is given, the doublet distribution function $g(\lambda,y)$ of frequency $\lambda/2\pi$ can be obtained with equation (30). The function $g(\lambda,y)$ is independent of the pressure distribution of the neighboring chord. Furthermore, if $\lambda \longrightarrow 0$ in equation (30),

$$g(0,y) = \frac{1}{2\pi}\int_{-\infty}^{\infty} dtC_p(t,y,+0) \tag{31}$$

On the right side, $\int_{-\infty}^{\infty} dtC_p(t,y,+0)$ is equal to one-half of the lift-coefficient distribution, $\frac{-1}{2}\left(\frac{\partial C_L}{\partial y}\right)$, at y. Thus, $g(0,y)$ is equivalent to $\frac{-1}{4\pi}\left(\frac{\partial C_L}{\partial y}\right)$ at y which has a physical meaning.

Unfortunately, equation (23) of the doublet-sheet potential satisfies one of the boundary conditions on the wing, but does not satisfy the other required boundary condition that the potential and its derivatives must be zero far ahead of the body. In other words, the correct potential must be zero as $t \longrightarrow -\infty$.

The potential of the doublet sheet at large $\pm t$ is investigated as follows. Introduce $\nu = \lambda t$ into equation (23):

$$\phi(t,y,z) = \mathrm{Re}\left[-2m'U\int_{-\infty}^{\infty} d\eta \int_{0}^{\infty} \frac{d\nu}{t}\, g\left(\frac{\nu}{t},\eta\right) e^{i\nu} H_1^{(2)}\left(\frac{\nu r}{t}\right)\frac{z}{r}\right] \tag{32}$$

For very large values of t there can be written

$$H_1^{(2)}\left(\frac{\nu r}{t}\right) \approx \frac{2it}{\pi\nu r}$$

and

$$g\left(\frac{\nu}{t},\eta\right) \approx g(0,\eta)$$

$$\lim_{t\longrightarrow\pm\infty} \phi_1(t,y,z) = \lim_{t\longrightarrow\pm\infty} \mathrm{Re}\left[\frac{-4m'Ui}{\pi}\int_{-\infty}^{\infty}\frac{z}{r^2}\,d\eta g(0,\eta)\int_0^{\infty}\frac{e^{i\nu}}{\nu}\,d\nu\right]$$

$$= \lim_{t\longrightarrow\pm\infty}\left[\frac{4m'U}{\pi}\int_{-\infty}^{\infty}\frac{z}{r^2}\,d\eta g(0,\eta)\int_0^{\infty}\frac{\sin\nu}{\nu}\,d\nu\right]$$

$$\phi_1(\pm\infty,y,z) = \chi^* = \pm 2m'U\int_{-\infty}^{\infty}\frac{z}{r^2}\,d\eta g(0,\eta) \tag{33}$$

where the negative sign corresponds to $t = -\infty$ and the positive sign corresponds to $t = \infty$. As $\chi^*(y,z)$ is independent of t, it satisfies the Laplace equation $\frac{\partial^2\chi^*}{\partial x^2} + \frac{\partial^2\chi^*}{\partial y^2} = 0$ and can be added to ϕ, the doublet-sheet potential, without an effect on the pressure distribution. It should be noted that the value of the potential function as $t \to \infty$ is $2\chi^*$. Hence χ^* may be interpreted physically as the potential function of the downwash in the Trefftz plane.

Thus, from equations (24) and (33) the complete solution of the present problem on supersonic wing lift is

$$\phi(t,y,z) = \phi_1 + \chi^* = m'U \int_{-\infty}^{\infty} \frac{z}{r^2}\, d\eta \left[2g(0,\eta) - \int_{-\infty}^{\infty} r\, d\lambda g(\lambda,\eta) e^{i\lambda t} H_1^{(2)}(\lambda r) \right] \tag{34}$$

In the case where C_p is given, the above equation can be written, with equations (30) and (31),

$$\phi(t,y,z) = \frac{m'U}{2\pi} \int_{-\infty}^{\infty} \frac{z}{r^2}\, d\eta \int_{-\infty}^{\infty} d\tau C_p(\tau,\eta,+0) \left[2 - \int_{-\infty}^{\infty} r\, d\lambda e^{i\lambda(t-\tau)} H_1^{(2)}(\lambda r) \right] \tag{35}$$

Let $\lambda r = \nu$; then

$$\phi(t,y,z) = \frac{m'U}{2\pi} \int_{-\infty}^{\infty} \frac{z}{r^2}\, d\eta \int_{-\infty}^{\infty} d\tau C_p(\tau,\eta,+0) \left[2 - \int_{-\infty}^{\infty} d\nu e^{i\nu\left(\frac{t-\tau}{r}\right)} H_1^{(2)}(\nu) \right] \tag{36}$$

With reference 18, page 405, the bracketed term in equation (36) can be evaluated as

$$2 - \int_{-\infty}^{\infty} d\nu e^{i\nu\left(\frac{t-\tau}{r}\right)} H_1^{(2)}(\nu) = \begin{cases} 0 & \frac{t-\tau}{r} \leq 1 \\ \dfrac{4}{\sqrt{1 - \left(\frac{r}{t-\tau}\right)^2}} & \frac{t-\tau}{r} > 1 \end{cases} \tag{37}$$

Thus, if the vortex of the foremost Mach cone is taken as the origin, there can be written

$$\phi(t,y,z) = \frac{2m'U}{\pi} \int_{-\infty}^{\infty} \frac{z}{r^2}\, d\eta \int_{-\infty}^{t-r} d\tau\, \frac{(t - \tau)C_p(\tau,\eta,+0)}{\sqrt{(t - \tau)^2 - r^2}} \tag{38}$$

which is the equation of the potential in terms of the pressure coefficient on the wing. The value of C_p is zero outside the wing. Since the radical must be positive, ϕ is zero outside the foremost Mach cone, as predicated by other theories.

AERODYNAMIC BEHAVIOR OF SYMMETRICAL FLAT BODIES IN SUPERSONIC FLOW

As the disturbance potential for the symmetrical flat body in supersonic flow has been given in equation (15b), with the Fourier integral method, the present section will show the expression for the pressure coefficient and the wave drag of various types of wing plan forms and airfoil sections.

Derivation of the Expression for the Wave Drag of a Wing

To the order of approximation of the linearized theory, the increment of pressure Δp anywhere within the disturbance area is

$$\Delta p = p - p_o = -\rho U u = -\rho_o U \frac{\partial \phi_o}{\partial x} = -\frac{\rho_o U}{m'} \frac{\partial \phi_o}{\partial t} \tag{39}$$

where the relations $x = \left(M^2 - 1\right)^{1/2} t = m't$ and $u = \partial\phi_o/\partial x$ are used, p and ρ are the local pressure and density, respectively, at the point $(x,y,\pm z)$, and p_o and ρ_o are the free-stream pressure and density, respectively.

To find $\partial\phi_o/\partial t$, equation (15b) can be differentiated as

$$\frac{u}{m'} = \frac{\partial \phi_o}{\partial t} = \frac{U}{2} \int_{-\infty}^{\infty} d\eta \int_{-\infty}^{\infty} \lambda\, d\lambda f(\lambda,\eta) e^{i\lambda t} H_0^{(2)}(\lambda r) \tag{40}$$

where $\partial\phi_o/\partial t$ is an even function with respect to z.

Substituting equation (40) into equation (39),

$$\Delta p(x,y,z) = \frac{\rho_o U^2}{2m'} \int_{-\infty}^{\infty} d\eta \int_{-\infty}^{\infty} \lambda \, d\lambda f(\lambda,\eta) e^{i\lambda t} H_0^{(2)}(\lambda r) \tag{41}$$

If the pressure increment on the wing surface which is located equivalently at $z = +0$ is desired, $r \longrightarrow |y - \eta|$ and

$$\Delta p(t,y,\pm 0) = \frac{\rho_o U^2}{2m'} \int_{-\infty}^{\infty} d\eta \int_{-\infty}^{\infty} \lambda \, d\lambda f(\lambda,\eta) e^{i\lambda t} H_0^{(2)}(\lambda|y - \eta|) \tag{42}$$

If it is the wave drag distribution along the span $\partial D/\partial y$ which is of interest, all the horizontal components of the pressure increment along the x- or t-direction on both the top and bottom surfaces over a unit span width must be summed up. Mathematically,

$$\left(\frac{\partial D}{\partial y}\right)_y = 2 \int_{-\infty}^{\infty} \Delta p \alpha_o \, dx \tag{43}$$

where α_o is the surface slope of the airfoil along the line of constant y as given in equation (18). With the expression for $\alpha_o(t,y,+0)$ and $\Delta p(t,y,+0)$ in equation (42), the drag distribution per unit span can be determined as

$$\frac{\partial D}{\partial y} = \rho_o U^2 \int_{-\infty}^{\infty} d\eta \int_{-\infty}^{\infty} \lambda \, d\lambda H_o^{(2)}(\lambda|y-\eta|) f(\lambda,\eta) \int_{-\infty}^{\infty} dt \int_{-\infty}^{\infty} d\lambda' e^{i(\lambda+\lambda')t} f(\lambda',y) \tag{44}$$

where λ' and y correspond to α_o. To evaluate the last double integral, write $\lambda' = -\lambda''$ and the double integral can be written as

$$\int_{-\infty}^{\infty} dt \int_{-\infty}^{\infty} d\lambda' e^{i(\lambda+\lambda')t} f(\lambda',y) = \int_{-\infty}^{\infty} dt \int_{-\infty}^{\infty} (-d\lambda'') e^{i(\lambda-\lambda'')t} f(-\lambda'',y)$$

$$= \int_{-\infty}^{\infty} dt \int_{-\infty}^{\infty} d\lambda'' e^{i(\lambda-\lambda'')t} \overline{f(\lambda'',y)} \qquad (45)$$

where

$$f(-\lambda'',y) = f_0(-\lambda'',y) + if_1(-\lambda'',y)$$

$$= f_0(\lambda'',y) - if_1(\lambda'',y)$$

$$= \overline{f(\lambda'',y)}$$

is introduced because f_0 is even and f_1 is odd. From the complex Fourier integral theorem,

$$2\pi\overline{f(\lambda,y)} = \int_{-\infty}^{\infty} dt \int_{-\infty}^{\infty} d\lambda'' e^{i(\lambda-\lambda'')t} \overline{f(\lambda'',y)} \qquad (46)$$

if the Lebesgue integral $\int_{-\infty}^{\infty} d\lambda'' \left|\overline{f(\lambda'',y)}\right| < \infty$ exists or if $\overline{f(\lambda'',y)}$ is of bounded variation, in the neighborhood $\lambda = \lambda''$. (See theorem 23, reference 19, p. 42.) Substituting equation (46) into equation (44) gives.

$$\left(\frac{\partial D}{\partial y}\right)_y = 2\pi\rho_o U^2 \int_{-\infty}^{\infty} d\eta \int_{-\infty}^{\infty} \lambda\, d\lambda H_0^{(2)}(\lambda|y - \eta|) f(\lambda,\eta)\overline{f(\lambda,y)}$$

$$= 2\pi\rho_o U^2 \int_{-\infty}^{\infty} d\eta \int_{-\infty}^{\infty} \lambda\, d\lambda \Big[H_0^{(2)}(\lambda|y - \eta|) f(\lambda,\eta)\overline{f(\lambda,y)} +$$

$$\overline{H_0^{(2)}(\lambda|y - \eta|)}\,\overline{f(\lambda,\eta)} f(\lambda,y)\Big]$$

$$= 2\pi\rho_o U^2 \int_{-\infty}^{\infty} d\eta \int_{0}^{\infty} \lambda\, d\lambda \Big\{J_0(\lambda|y - \eta|)\big[f_0(\lambda,\eta) f_0(\lambda,y) +$$

$$f_1(\lambda,\eta) f_1(\lambda,y)\big] + Y_0(\lambda|y - \eta|)\big[f_1(\lambda,\eta) f_0(\lambda,y) - f_0(\lambda,\eta) f_1(\lambda,y)\big]\Big\} \tag{47}$$

where the relations

$$H_0^{(2)}(-\lambda|y - \eta|) = \overline{H_0^{(2)}(\lambda|y - \eta|)} = J_0(\lambda|y - \eta|) - iY_0(\lambda|y - \eta|)$$

$$f(-\lambda,\eta)\overline{f(-\lambda,y)} = \overline{f(\lambda,\eta)} f(\lambda,y)$$

are used so that the integration limit changes from 0 to ∞ instead of $-\infty$ to ∞. The imaginary part automatically cancels out.

Now, if D, the wave drag of the whole wing system, is desired, equation (47) can be integrated with respect to y:

$$D = \int_{-\infty}^{\infty} \left(\frac{\partial D}{\partial y}\right) dy = 2\pi\rho_o U^2 \int_{-\infty}^{\infty} dy \int_{-\infty}^{\infty} d\eta \int_{-\infty}^{\infty} \lambda\, d\lambda H_0^{(2)}(\lambda|y - \eta|) f(\lambda,\eta)\overline{f(\lambda,y)}$$

$$= 4\pi\rho_o U^2 \int_{-\infty}^{\infty} dy \int_{-\infty}^{\infty} d\eta \int_{0}^{\infty} \lambda\, d\lambda \Big\{J_0(\lambda|y - \eta|)\big[f_0(\lambda,\eta) f_0(\lambda,y) +$$

$$f_1(\lambda,\eta) f_1(\lambda,y)\big] + Y_0(\lambda|y - \eta|)\big[f_1(\lambda,\eta) f_0(\lambda,y) - f_0(\lambda,\eta) f_1(\lambda,y)\big]\Big\} \tag{48}$$

Now, as the wave drag D is independent of y and η, it should be independent of the order of integration or of the interchange of y with η. In carrying out such an interchange,

$$D' = 4\pi\rho_0 U^2 \int_{-\infty}^{\infty} d\eta \int_{-\infty}^{\infty} dy \int_0^{\infty} \lambda \, d\lambda \left\{ J_0(\lambda|\eta - y|) \left[f_0(\lambda,y) f_0(\lambda,\eta) + f_1(\lambda,y) f_1(\lambda,\eta) \right] + Y_0(\lambda|\eta - y|) \left[f_1(\lambda,y) f_0(\lambda,\eta) - f_0(\lambda,y) f_1(\lambda,\eta) \right] \right\}$$

This shows that the necessary condition $D = D'$ is

$$\int_{-\infty}^{\infty} d\eta \int_{-\infty}^{\infty} dy \int_0^{\infty} \lambda \, d\lambda \left\{ Y_0(\lambda|y - \eta|) \left[f_1(\lambda,y) f_0(\lambda,\eta) - f_1(\lambda,\eta) f_0(\lambda,y) \right] \right\} = 0 \tag{49}$$

This is one of the important relations that has been developed by Von Kármán.

There is another way of evaluating the wave drag as pointed out by Von Kármán. The total momentum transfer through a cylindrical surface of very large radius R which contains the wing in the flight direction must be equal to the wave drag, by means of Newton's laws. Thus,

$$D = -\rho_0 \int_{-\infty}^{\infty} dt \int_0^{2\pi} R \, d\theta \, \frac{\partial \phi}{\partial r} \frac{\partial \phi}{\partial t} \tag{50}$$

which is the same as equation (48). Applying equation (49), equation (48) can be written as

$$D = 4\pi\rho_0 U^2 \int_{-\infty}^{\infty} dy \int_{-\infty}^{\infty} d\eta \int_0^{\infty} \lambda \, d\lambda J_0(\lambda|y - \eta|) \left[f_0(\lambda,\eta) f_0(\lambda,y) + f_1(\lambda,\eta) f_1(\lambda,y) \right] \tag{51}$$

In the case of a sweptback wing which is symmetrical with respect to the x,z-plane, $f_0(\lambda,y)$ and $f_1(\lambda,y)$ are even functions with respect to y. To take care of this point, write

$$D = 4\pi\rho_o U^2 \int_{-\infty}^{\infty} dy \int_{-\infty}^{\infty} d\eta \int_0^{\infty} \lambda\, d\lambda J_0(\lambda|y - \eta|)\left[f_0(\lambda,|\eta|)f_0(\lambda,|y|) + f_1(\lambda,|\eta|)f_1(\lambda,|y|)\right]$$

$$= 4\pi\rho_o U^2 \int_{-\infty}^{\infty} dy \int_0^{\infty} d\eta \int_0^{\infty} \lambda\, d\lambda \left\{J_0(\lambda|y - \eta|) + J_0\left[\lambda(y + \eta)\right]\right\}\left[f_0(\lambda,\eta)f_0(\lambda,|y|) + f_1(\lambda,\eta)f_1(\lambda,|y|)\right]$$

$$= 8\pi\rho_o U^2 \int_0^{\infty} dy \int_0^{\infty} d\eta \int_0^{\infty} \lambda\, d\lambda \left\{J_0(\lambda|y - \eta|) + J_0\left[\lambda(y + \eta)\right]\right\}\left[f_0(\lambda,\eta)f_0(\lambda,y) + f_1(\lambda,\eta)f_1(\lambda,y)\right] \tag{52}$$

where the limits of η and y change as shown. Equation (52) will be used in the next section very often. If the span is finite (say that b is the semispan) and the airfoil sections are similar everywhere, equation (52) can be written

$$D = 8\pi\rho_o U^2 \int_0^{b} dy \int_0^{b} d\eta \int_0^{\infty} \lambda\, d\lambda \left\{J_0(\lambda|y - \eta|) + J_0\left[\lambda(y + \eta)\right]\right\}\left[f_0(\lambda,\eta)f_0(\lambda,y) + f_1(\lambda,\eta)f_1(\lambda,y)\right] \tag{53}$$

Wave Drag of a Tapered Sweptback Wing

If the double-wedge profile is taken as the airfoil section of the wing as shown in appendix A, and equation (A8) is introduced into equation (53), there results

$$D = 8\pi\rho_o U^2 \int_0^b dy \int_0^b d\eta \int_0^\infty \lambda\, d\lambda \left\{ J_0(\lambda|y - \eta|) + J_0\left[\lambda(y + \eta)\right] \right\} \frac{(\alpha_o')^2}{\pi^2\lambda^2}(1 - \cos \lambda a_y')(1 - \cos \lambda a_\eta') \cos \lambda\beta(|y| - |\eta|)$$

$$= \frac{8\rho_o U^2 (\alpha_o')^2}{\pi} \int_0^b dy \int_0^b d\eta \int_0^\infty \frac{d\lambda}{\lambda} \left\{ J_0(\lambda|y - \eta|) + J_0\left[\lambda(y + \eta)\right] \right\} (1 - \cos \lambda a_y')(1 - \cos \lambda a_\eta') \cos \lambda\beta(|y| - |\eta|) \qquad (54)$$

By definition,

$$\left.\begin{aligned} b' &= \frac{b}{a_o'} \qquad y' = \frac{y}{a_o'} \qquad \eta' = \frac{\eta}{a_o'} \qquad \nu' = \frac{\nu}{m'} \\ a_y' &= a_o'(1 - \nu' y') \\ a_\eta' &= a_o'(1 - \nu' \eta') \end{aligned}\right\} \qquad (55)$$

For details of the notation refer to figure 1 and appendix B.

The wave drag equation can be written in another form

$$\frac{\pi D}{8\rho_o U^2(\alpha_o')^2(a_o')^2} = \int_0^{b'} dy' \int_0^{b'} d\eta' \int_0^{\infty} \frac{d\lambda}{\lambda} \left\{ J_0\left[(\eta' - y')\lambda a_o'\right] + J_0\left[(\eta' + y')\lambda a_o'\right] \right\} \left(-\frac{1}{4}\left\{ 1 - \cos \lambda a_o'\left[2 + \beta(\eta' - y') - \nu'(\eta' + y')\right] \right\} - \frac{1}{4}\left\{ 1 - \cos \lambda a_o'\left[2 - \beta(\eta' - y') - \nu'(\eta' + y')\right] \right\} - \frac{1}{4}\left[1 - \cos \lambda a_o'(\beta + \nu')(\eta' - y')\right] - \frac{1}{4}\left\{ 1 - \cos \left[\lambda a'(\beta - \nu')(\eta' - y')\right] \right\} + \frac{1}{2}\left\{ 1 - \cos \lambda a_o'\left[1 + \beta(\eta' - y') - \nu' y'\right] \right\} + \frac{1}{2}\left\{ 1 - \cos \lambda a_o'\left[1 - \beta(\eta' - y') - \nu' y'\right] \right\} + \frac{1}{2}\left\{ 1 - \cos \lambda a_o'\left[1 + \beta(\eta' - y') - \nu'\eta'\right] \right\} + \frac{1}{2}\left\{ 1 - \cos \lambda a_o'\left[1 - \beta(\eta' - y') - \nu'\eta'\right] \right\} - \left[1 - \cos \beta\lambda a_o'(\eta' - y')\right] \right) \tag{56}$$

With the known infinite integrals of Bessel functions as shown in appendix C, the integration in equation (56) can be carried out.

$$\frac{\pi D}{8\rho_o U^2 (a_o')^2 (a_o')^2} = \int_0^{b'} dy' \int_0^{b'} d\eta' \left[-\frac{1}{4}\cosh^{-1}\frac{2+\beta(\eta'-y')-\nu'(\eta'+y')}{\eta'-y'} - \frac{1}{4}\cosh^{-1}\frac{2+\beta(\eta'-y')-\nu'(\eta'+y')}{\eta'+y'} - \right.$$

$$\frac{1}{4}\cosh^{-1}\frac{2-\beta(\eta'-y')-\nu'(\eta'+y')}{\eta'-y'} - \frac{1}{4}\cosh^{-1}\frac{2-\beta(\eta'-y')-\nu'(\eta'+y')}{\eta'+y'} -$$

$$\frac{1}{4}\cosh^{-1}\frac{(\beta+\nu')(\eta'-y')}{\eta'+y'} - \frac{1}{4}\cosh^{-1}(\beta+\nu') - \frac{1}{4}\cosh^{-1}(\beta-\nu') - \frac{1}{4}\cosh^{-1}\frac{(\beta-\nu')(\eta'-y')}{\eta'+y'} +$$

$$\frac{1}{2}\cosh^{-1}\frac{1+\beta(\eta'-y')-\nu'y'}{\eta'-y'} + \frac{1}{2}\cosh^{-1}\frac{1+\beta(\eta'-y')-\nu'y'}{\eta'+y'} + \frac{1}{2}\cosh^{-1}\frac{1-\beta(\eta'-y')-\nu'y'}{\eta'+y'} +$$

$$\frac{1}{2}\cosh^{-1}\frac{1-\beta(\eta'-y')-\nu'y'}{\eta'-y'} + \frac{1}{2}\cosh^{-1}\frac{1+\beta(\eta'-y')-\nu'\eta'}{\eta'-y'} + \frac{1}{2}\cosh^{-1}\frac{1+\beta(\eta'-y')-\nu'\eta'}{\eta'+y'} +$$

$$\left. \frac{1}{2}\cosh^{-1}\frac{1-\beta(\eta'-y')-\nu'\eta'}{\eta'-y'} + \frac{1}{2}\cosh^{-1}\frac{1-\beta(\eta'-y')-\nu'\eta'}{\eta'+y'} - \cosh^{-1}\frac{\beta(\eta'-y')}{\eta'+y'} - \cosh^{-1}\beta \right] \quad (57)$$

In all $\cosh^{-1}(A)$ terms, A must be positive. In order to carry out the integration, a transformation of the coordinate system may be introduced as follows: Let $u' = \eta' + y'$, $v' = \eta' - y'$. Then,

$$dy'\,d\eta' = \frac{\partial(y',\eta')}{\partial(u',v')}\,du'\,dv' = \frac{1}{2}\,du'\,dv'$$

$$y' = 0,\ \eta' = 0 \longrightarrow u' = 0,\ v' = 0$$

$$y' = 0,\ \eta' = b \longrightarrow u' = b,\ v' = b$$

$$y' = b,\ \eta' = 0 \longrightarrow u' = b,\ v' = -b$$

$$y' = b,\ \eta' = b \longrightarrow u' = 2b',\ v = 0$$

With this transformation, the square domain in the y',η'-plane will transform to a diamond-shaped domain (of twice the area) in the u',v'-plane.

$$\frac{\pi D}{8\rho_o U^2(a_o')^2(a_o')^2} = -(b')^2\left[\frac{1}{4}\cosh^{-1}(\beta+\nu') + \frac{1}{4}\cosh^{-1}(\beta-\nu') + \cosh^{-1}\beta\right] + \int_0^{b'} du' \int_0^{u'} dv' \left(\left[-\frac{1}{4}\cosh^{-1}\left(\frac{2-\nu'u'}{\nu'}+\beta\right) - \right.\right.$$

$$\frac{1}{4}\cosh^{-1}\left(\frac{2+\beta\nu'}{u'}-\nu'\right) - \frac{1}{4}\cosh^{-1}\left(\frac{2-\nu'u'}{\nu'}-\beta\right) - \frac{1}{4}\cosh^{-1}\left(\frac{2-\beta\nu'}{u'}-\nu'\right) - \frac{1}{4}\cosh^{-1}\frac{(\beta+\nu')\nu'}{u'} -$$

$$\left.\frac{1}{4}\cosh^{-1}\frac{(\beta-\nu')\nu'}{u'}\right] + \left[-\frac{1}{4}\cosh^{-1}\left(\frac{2-2\nu'b'+\nu'u'}{\nu'}+\beta\right) - \frac{1}{4}\cosh^{-1}\left(\frac{2+\beta\nu'}{2b'-u'}-\nu'\right) -$$

$$\frac{1}{4}\cosh^{-1}\left(\frac{2-2\nu'b'+\nu'u'}{\nu'}-\beta\right) - \frac{1}{4}\cosh^{-1}\left(\frac{2-\beta\nu'}{2b'-u'}-\nu'\right) - \frac{1}{4}\cosh^{-1}\frac{(\beta+\nu')\nu'}{2b'-u'} -$$

$$\frac{1}{4}\cosh^{-1}\frac{(\beta-\nu')\nu'}{2b'-u'}\Big] + \frac{1}{2}\left\{\cosh^{-1}\left(\frac{2-\nu'u'}{2\nu'}+\beta+\frac{\nu'}{2}\right) + \cosh^{-1}\left[\frac{2+(2\beta+\nu')\nu'}{2u'}-\frac{\nu'}{2}\right] + \right.$$

$$\cosh^{-1}\left(\frac{2-\nu'u'}{2\nu'}-\beta+\frac{\nu'}{2}\right) + \cosh^{-1}\left[\frac{2-(2\beta-\nu')\nu'}{2u'}-\frac{\nu'}{2}\right] + \cosh^{-1}\left(\frac{2-\nu'u'}{2\nu'}+\beta-\frac{\nu'}{2}\right) +$$

$$\left.\cosh^{-1}\left[\frac{2+(2\beta-\nu')\nu'}{2u'}-\frac{\nu'}{2}\right] + \cosh^{-1}\left(\frac{2-\nu'u'}{2\nu'}-\beta-\frac{\nu'}{2}\right) + \cosh^{-1}\left[\frac{2-(2\beta+\nu')\nu'}{2u'}-\frac{\nu'}{2}\right]\right\} +$$

$$\frac{1}{2}\left\{\cosh^{-1}\left(\frac{2-2\nu'b'+\nu'u'}{2\nu'}+\beta+\frac{\nu'}{2}\right) + \cosh^{-1}\left[\frac{2+(2\beta+\nu')\nu'}{2(2b'-u')}-\frac{\nu'}{2}\right] + \cosh^{-1}\left(\frac{2-2\nu'b'+\nu'u'}{2\nu'}-\beta+\frac{\nu'}{2}\right) + \right.$$

$$\cosh^{-1}\left[\frac{2-(2\beta-\nu')\nu'}{2(2b'-u')}-\frac{\nu'}{2}\right] + \cosh^{-1}\left(\frac{2-2\nu'b'+\nu'u'}{2\nu'}+\beta-\frac{\nu'}{2}\right) + \cosh^{-1}\left[\frac{2+(2\beta'-\nu')\nu'}{2(2b'-u')}-\frac{\nu'}{2}\right] +$$

$$\left.\cosh^{-1}\left(\frac{2-2\nu'b'+\nu'u'}{2\nu'}-\beta-\frac{\nu'}{2}\right) + \cosh^{-1}\left[\frac{2-(2\beta+\nu')\nu'}{2(2b'-u')}-\frac{\nu'}{2}\right]\right\} + \left(-\cosh^{-1}\frac{\beta\nu'}{u'} - \cosh^{-1}\frac{\beta\nu'}{2b'-u'}\right)\Bigg) \qquad (58)$$

The details of the integration are too complicated to be given here. The result can be summarized in equation (59) which follows, where $\beta_o = \beta + \nu'$, $\beta_1 = \beta - \nu'$, $\sigma = 1 - \nu'b'$, and $\sin^{-1}(A) = (\text{sign } A)\frac{\pi}{2}$ if $|A| > 1$. The upper line with $1 - \beta^2$ should be used, if $\beta < 1$; the lower line with $\beta^2 - 1$ should be used, if $\beta > 1$; and the signs of all $\cosh^{-1}$ terms should be reversed if $\beta < -1$. The above rules should be also applied for β_o and β_1. Therefore equation (59) covers all cases except a few limiting cases: $\beta = \pm 1$, $\beta_o = \pm 1$, $\beta_1 = \pm 1$, $\nu' = 0$, and $\beta = \infty$ (i.e., $M \rightarrow 1$). These limiting cases will be shown in the next section.

$$\frac{\pi}{2} b'(1+\sigma)\frac{C_D}{C_{D_o}} = (b')^2 \left\{ \left[-\frac{\beta_o}{2(\beta_o^2-1)^{1/2}} \cosh^{-1}\left|\frac{\beta_o^2+1}{2\beta_o}\right| \right]^a - \left[\frac{\beta_1}{2(\beta_1^2-1)^{1/2}} \cosh^{-1}\left|\frac{\beta_1^2+1}{2\beta_1}\right| \right]^b - \left[\frac{2\beta}{(\beta^2-1)^{1/2}} \cosh^{-1}\left|\frac{\beta^2+1}{2\beta}\right| \right]^c - \cosh^{-1}\frac{\sigma}{b'} + 4\cosh^{-1}\frac{\sigma}{2b'} \right\} +$$

$$\left\{ \begin{array}{l} \dfrac{(1+\beta_o b')^2}{2\beta(1-\beta_o^2)^{1/2}} \left[-\sin^{-1}\dfrac{\sigma\beta_o + b'}{1+\beta b'} + \sin^{-1}\left[\beta_o + \dfrac{(1-\beta_o^2)b'}{2(1+\beta_o b')}\right] \right] + \dfrac{(\sigma + 2\beta_o b')^2}{2(\beta_o+\beta)(1-\beta_o^2)^{1/2}} \left\{ \sin^{-1}\dfrac{\sigma\beta_o + 2b'}{\sigma + 2\beta_o b'} - \sin^{-1}\left[\beta_o + \dfrac{(1-\beta_o^2)b'}{\sigma + 2\beta_o b'}\right] \right\} \\ \dfrac{(1+\beta_o b')^2}{2\beta(\beta_o^2-1)^{1/2}} \left[\cosh^{-1}\left|\dfrac{\sigma\beta_o + b'}{1+\beta b'}\right| - \cosh^{-1}\left|\beta_o + \dfrac{(1-\beta_o^2)b'}{2(1+\beta_o b')}\right| \right] + \dfrac{(\sigma + 2\beta_o b')^2}{2(\beta_o+\beta)(\beta_o^2-1)^{1/2}} \left[-\cosh^{-1}\left|\dfrac{\sigma\beta_o + 2b'}{\sigma + 2\beta_o b'}\right| + \cosh^{-1}\left|\beta_o + \dfrac{(1-\beta_o^2)b'}{\sigma + 2\beta_o b'}\right| \right] \end{array} \right\}^A +$$

$$\left\{ \begin{array}{l} \dfrac{(1-\beta_1 b')^2}{2\beta(1-\beta_1^2)^{1/2}} \left[-\sin^{-1}\dfrac{\sigma\beta_1 - b'}{1-\beta b'} + \sin^{-1}\left[\beta_1 - \dfrac{(1-\beta_1^2)b'}{2(1-\beta_1 b')}\right] \right] + \dfrac{(\sigma - 2\beta_1 b')^2}{2(\beta_1+\beta)(1-\beta_1^2)^{1/2}} \left\{ \sin^{-1}\dfrac{\sigma\beta_1 - 2b'}{\sigma - 2\beta_1 b'} - \sin^{-1}\left[\beta_1 - \dfrac{(1-\beta_1^2)b'}{\sigma - 2\beta b'}\right] \right\} \\ \dfrac{(1-\beta_1 b')^2}{2\beta(\beta_1^2-1)^{1/2}} \left[\cosh^{-1}\left|\dfrac{\sigma\beta_1 - b'}{1-\beta b'}\right| - \cosh^{-1}\left|\beta_1 - \dfrac{(1-\beta_1^2)b'}{2(1-\beta b')}\right| \right] + \dfrac{(\sigma - 2\beta_1 b')^2}{2(\beta_1+\beta)(\beta_1^2-1)^{1/2}} \left[-\cosh^{-1}\left|\dfrac{\sigma\beta_1 - 2b'}{\sigma - 2\beta_1 b'}\right| + \cosh^{-1}\left|\beta_1 - \dfrac{(1-\beta_1^2)b'}{\sigma - 2\beta b'}\right| \right] \end{array} \right\}^B +$$

$$\left\{ \begin{array}{l} \dfrac{(\sigma - 2\beta b')^2}{2(\beta_o+\beta)(1-\beta^2)^{1/2}} \left\{ \sin^{-1}\dfrac{\sigma\beta - 2b'}{\sigma - 2\beta b'} - \sin^{-1}\left[\beta - \dfrac{(1-\beta^2)b'}{\sigma - 2\beta b'}\right] \right\} + \dfrac{(\sigma + 2\beta b')^2}{2(\beta_1+\beta)(1-\beta^2)^{1/2}} \left\{ \sin^{-1}\dfrac{\sigma\beta + 2b'}{\sigma + 2\beta b'} - \sin^{-1}\left[\beta + \dfrac{(1-\beta^2)b'}{\sigma + 2\beta b'}\right] \right\} \\ \dfrac{(\sigma - 2\beta b')^2}{2(\beta_o+\beta)(\beta^2-1)^{1/2}} \left[-\cosh^{-1}\left|\dfrac{\sigma\beta - 2b'}{\sigma - 2\beta b'}\right| + \cosh^{-1}\left|\beta - \dfrac{(1-\beta^2)b'}{\sigma - 2\beta b'}\right| \right] + \dfrac{(\sigma + 2\beta b')^2}{2(\beta_1+\beta)(\beta^2-1)^{1/2}} \left[-\cosh^{-1}\left|\dfrac{\sigma\beta + 2b'}{\sigma + 2\beta b'}\right| + \cosh^{-1}\left|\beta + \dfrac{(1-\beta^2)b'}{\sigma + 2\beta b'}\right| \right] \end{array} \right\}^C +$$

$$\left\{ \begin{array}{l} \dfrac{1}{2\nu'(1-\beta_o^2)^{1/2}} \left[-\sigma^2 \sin^{-1}\left[\beta_o - \dfrac{(1-\beta_o^2)b'}{2\sigma}\right] + \sigma^2 \sin^{-1}\left[\beta_o - \dfrac{(1-\beta_o^2)b'}{\sigma}\right] - \dfrac{\beta_1}{\beta}\sin^{-1}\left[\beta_o + (1-\beta_o^2)\dfrac{b'}{2}\right] + \dfrac{2\beta}{\beta_o+\beta}\sin^{-1}\left[\beta_o + (1-\beta_o^2)b'\right] - \dfrac{\beta_o(\beta_o-\beta)}{\beta(\beta_o+\beta)}\sin^{-1}\beta_o \right] \\ \dfrac{1}{2\nu'(\beta_o^2-1)^{1/2}} \left[\sigma^2 \cosh^{-1}\left|\beta_o - \dfrac{(1-\beta_o^2)b'}{2\sigma}\right| - \sigma^2 \cosh^{-1}\left|\beta_o - \dfrac{(1-\beta_o^2)b'}{\sigma}\right| + \dfrac{\beta_1}{\beta}\cosh^{-1}\left|\beta_o + (1-\beta_o^2)\dfrac{b'}{2}\right| - \dfrac{2\beta}{\beta_o+\beta}\cosh^{-1}\left|\beta_o + (1-\beta_o^2)b'\right| + \dfrac{\beta_o(\beta_o-\beta)}{\beta(\beta_o+\beta)}\cosh^{-1}|\beta_o| \right] \end{array} \right\}^D +$$

$$\left\{ \begin{array}{l} \dfrac{1}{2\nu'(1-\beta_1^2)^{1/2}} \left\{ \sigma^2 \sin^{-1}\left[\beta_1 + \dfrac{(1-\beta_1^2)b'}{2\sigma}\right] - \sigma^2 \sin^{-1}\left[\beta_1 + \dfrac{(1-\beta_1^2)b'}{\sigma}\right] + \dfrac{\beta_o}{\beta}\sin^{-1}\left[\beta_1 - (1-\beta_1^2)\dfrac{b'}{2}\right] - \dfrac{2\beta}{(\beta_1+\beta)}\sin^{-1}\left[\beta_1 - (1-\beta_1^2)b'\right] + \dfrac{\beta_1(\beta-\beta_1)}{\beta(\beta_1+\beta)}\sin^{-1}\beta_1 \right\} \\ \dfrac{1}{2\nu'(\beta_1^2-1)^{1/2}} \left[-\sigma^2 \cosh^{-1}\left|\beta_1 + \dfrac{(1-\beta_1^2)b'}{2\sigma}\right| + \sigma^2 \cosh^{-1}\left|\beta_1 + \dfrac{(1-\beta_1^2)b'}{\sigma}\right| - \dfrac{\beta_o}{\beta}\cosh^{-1}\left|\beta_1 - (1-\beta_1^2)\dfrac{b'}{2}\right| + \dfrac{2\beta}{(\beta_1+\beta)}\cosh^{-1}\left|\beta_1 - (1-\beta_1^2)b'\right| - \dfrac{\beta_1(\beta-\beta_1)}{\beta(\beta_1+\beta)}\cosh^{-1}|\beta_1| \right] \end{array} \right\}^E +$$

$$\left\{ \begin{array}{l} \dfrac{1}{2\nu'(1-\beta^2)^{1/2}} \left\{ \sigma^2 \sin^{-1}\left[\beta - \dfrac{(1-\beta^2)b'}{2\sigma}\right] - \sigma^2 \sin^{-1}\left[\beta - \dfrac{(1-\beta^2)b'}{\sigma}\right] + \dfrac{2\beta_1}{\beta_1+\beta}\sin^{-1}\left[\beta + (1-\beta^2)b'\right] - \dfrac{2\beta_o}{\beta_o+\beta}\sin^{-1}\left[\beta + (1-\beta^2)b'\right] + \dfrac{4\beta(\beta_o-\beta)}{(\beta_o+\beta)(\beta_1+\beta)}\sin^{-1}\beta \right\} \\ \dfrac{1}{2\nu'(\beta^2-1)^{1/2}} \left[-\sigma^2 \cosh^{-1}\left|\beta - \dfrac{(1-\beta^2)b'}{2\sigma}\right| + \sigma^2 \cosh^{-1}\left|\beta - \dfrac{(1-\beta^2)b'}{\sigma}\right| - \dfrac{2\beta_1}{\beta_1+\beta}\cosh^{-1}\left|\beta + (1-\beta^2)b'\right| + \dfrac{2\beta_o}{\beta_o+\beta}\cosh^{-1}\left|\beta + (1-\beta^2)b'\right| - \dfrac{4\beta(\beta_o-\beta)}{(\beta_o+\beta)(\beta_1+\beta)}\cosh^{-1}|\beta| \right] \end{array} \right\}^F \qquad (59)$$

where a, b, c, A, B, C, D, E, and F designate the terms to be used in the next section.

For a given sweptback wing, $\beta_o > 1$, $= 1$, or < 1 means the Mach line ahead, on, or behind the leading edge, respectively; $\beta_1 > 1$, $= 1$, or < 1 means the Mach line ahead, on, or behind the trailing edge. With a fixed taper ratio, the trailing edge may be swept forward; $\beta_1 = -1$ means the sweptforward trailing edge coincides with the Mach line. Similarly, β refers to the midchord or the line of the maximum thickness. At all β's equal to $|1|$ there occurs a discontinuity of the slope of the curve of the wave drag. In other words, curves for $\beta = |1|$ are the envelopes of cusps of the C_D/C_{D_o} curves at constant β.

To demonstrate the use of these results, the wave drag coefficients of two families of sweptback wings have been calculated as shown in figures 2 and 3 with taper ratios of 0.2 and 0.5, respectively. The essential parameters are C_D/C_{Do}, A tan Λ, and β. The effect of the Mach number is contained in $\beta = \tan \Lambda/m'$ and $C_{Do} = 4\alpha_o^2/m'$, the two-dimensional wave drag coefficient of Ackeret. To use these curves, first fix the sweptback angle Λ and aspect ratio. Of course, σ will have to be chosen as 0.2 or 0.5 in order to use these graphs. Then, with a fixed A tan Λ, read off C_D/C_{Do} at various values of β along the fixed abscissa. Replotting C_D/C_{Do} against β, the example shown in figure 4, actually gives a family of swept wings of fixed A tan Λ. The curve of C_D against Mach number can be plotted from the relation $M = \sqrt{\left(\frac{\tan \Lambda}{\beta}\right)^2 + 1}$. This is not given in this report.

It is very interesting to note that $\left(C_D/C_{Do}\right)_{max}$ occurs when the Mach line coincides with the leading edge, $\beta_o = 1$, or the line of maximum thickness, $\beta = 1$. In figure 2 ($\sigma = 0.2$), $\left(C_D/C_{Do}\right)_{max}$ occurs at $\beta = 1$ for A tan $\Lambda > 7.5$ approximately, and at $\beta_o = 1$ for A tan $\Lambda < 7.5$. In figure 3 ($\sigma = 0.5$), $\left(C_D/C_{Do}\right)_{max}$ occurs always at $\beta_o = 1$ except for A tan $\Lambda < 2/3$. Also, C_D/C_{Do} increases monotonically with A tan Λ at $\beta_o = 1$, $\beta = 1$, or $\beta_1 = 1$, but decreases monotonically with A tan Λ for $\beta_1 = -1$.

Figure 5 shows β corresponding to $\beta_o = 1$ and $\beta_1 = 1$ plotted against A tan Λ. This is needed for locating the cusp of the curve of C_D/C_{Do} against β, as shown in figure 4. These curves are obtained from the relations:

$$\beta_1 = \beta\left[1 - \frac{2(1 - \sigma)}{(1 + \sigma)A \tan \Lambda}\right]$$

$$\beta_o = \beta\left[1 + \frac{2(1 - \sigma)}{(1 + \sigma)(A \tan \Lambda)}\right]$$

A few interesting facts can be drawn from figures 2 and 3, although the taper ratios are fixed at 0.2 and 0.5, respectively. First, if $\beta = \tan \Lambda/m' = 0$, $M \longrightarrow \infty$ for $\Lambda \neq 0$, or $\Lambda = 0$ for $M > 1$. For $\Lambda \neq 0$, $C_D/C_{Do} = 1$ or $C_D = C_{Do}$ as indicated. For $\Lambda = 0$, $0 < C_D/C_{Do} \leq 1$ and the exact value of C_D/C_{Do} is indeterminate. As β increases from 0 to 1, C_D/C_{Do} rises quickly with $A \tan \Lambda$ until it meets the curves $\beta_o = 1$ and then varies with $A \tan \Lambda$ very slowly. At $\beta = 1$, C_D/C_{Do} is extremely high. This means that the closer the Mach line to the maximum-thickness line, the higher the drag. As β increases further, from $1 \longrightarrow \infty$, C_D/C_{Do} decreases with increasing β. This means that the closer the Mach line to the maximum-thickness line, the higher the drag also.

If the sweptback angle is negative, or if the flow direction is reversed, the curve of C_D/C_{Do} against $-A \tan |\Lambda|$ is actually the reflection of the present curves with the following changes: $\beta \longrightarrow -\beta$, $\beta_o = 1 \longrightarrow \beta_1 = -1$, $\beta_1 = 1 \longrightarrow \beta_o = -1$, and $\beta_1 = -1 \longrightarrow \beta_o = 1$ if β_o is defined as corresponding to the leading edge, and β_1 as corresponding to the trailing edge. It will be found that C_D/C_{Do} depends only on $A \tan |\Lambda|$ and $|\beta|$ for the same wing whether it flies forward or backward. This confirms the reversed-flow theorem in references 2 and 5.

Special Cases of the Wave Drag Equation

Most of the special cases of the wave drag equation are required in calculating the curves shown in figures 2 and 3 and therefore must be written down one by one. These special cases are based upon the taper ratio that is between 0 and 1.

(a) As $\beta_o \longrightarrow 1$, expressions A and D in equation (58) take on the following limiting values while the rest of the equation stays the same except $a = b = c = 0$.

$$A = \frac{(1 - \nu'b' + b')^2}{2(\nu' - 1)}\left[-\left(\frac{1 - \nu'b' - b'}{1 - \nu'b' + b'}\right)^{1/2} + \left(\frac{1 - \nu'b'}{1 - \nu'b' + b'}\right)^{1/2}\right] + \frac{(1 - \nu'b' + 2b')^2}{2(\nu' - 2)}\left[\left(\frac{1 - \nu'b' - 2b'}{1 - \nu'b' + 2b'}\right)^{1/2} - \left(\frac{1 - \nu'b'}{1 - \nu'b' + 2b'}\right)\right]$$

$$D = \frac{1}{2\nu'}\left\{\sigma^{3/2}\left[(1 - \nu'b' + b')^{1/2} - (1 - \nu'b' + 2b')^{1/2}\right] + \frac{2\nu' - 1}{\nu' - 1}(1 - b')^{1/2} - \frac{2(\nu' - 1)}{\nu' - 2}(1 - 2b')^{1/2} + \frac{\nu'}{(\nu' - 1)(\nu' - 2)}\right\} \tag{60}$$

This case occurs when the right characteristic coincides with the leading edge on the right side.

(b) Similarly, for $\beta_1 = 1$, expressions B and E become

$$B = \frac{(1 - \nu'b' - b')^2}{2(\nu' + 1)}\left[\left(\frac{1 - \nu'b' + b'}{1 - \nu'b' - b'}\right)^{1/2} - \left(\frac{1 - \nu'b'}{1 - \nu'b' - b'}\right)^{1/2}\right] + \frac{(1 - \nu'b' - 2b')^2}{2(\nu' + 2)}\left[-\left(\frac{1 - \nu'b' + 2b'}{1 - \nu'b' - 2b'}\right)^{1/2} + \left(\frac{1 - \nu'b'}{1 - \nu'b' - 2b'}\right)^{1/2}\right]$$

$$E = \frac{1}{2\nu'}\left\{\sigma^{3/2}\left[-(1 - \nu'b' - b')^{1/2} + (1 - \nu'b' - 2b')^{1/2}\right] - \frac{2\nu' + 1}{\nu' + 1}(1 + b')^{1/2} + \frac{2(\nu' + 1)}{\nu' + 2}(1 + 2b')^{1/2} + \frac{\nu'}{(\nu' + 1)(\nu' + 2)}\right\} \tag{61}$$

Here $b = 0$. All the other terms remain the same as shown in equation (59). This case occurs when the right characteristic coincides with the trailing edge on the right side.

(c) When $\beta = 1$, the expressions C and F are

$$\left.\begin{aligned} C = {} & \frac{(\sigma + 2b')^2}{2(2 - \nu')}\left[-\left(\frac{\sigma - 2b'}{\sigma + 2b'}\right)^{1/2} + \left(\frac{\sigma}{\sigma + 2b'}\right)^{1/2}\right] + \\ & \frac{(\sigma - 2b')^2}{2(2 + \nu')}\left[-\left(\frac{\sigma + 2b'}{\sigma - 2b'}\right)^{1/2} + \left(\frac{\sigma}{\sigma - 2b'}\right)^{1/2}\right] \\ F = {} & \frac{1}{2\nu'}\left\{\sigma^{3/2}\left[-(\sigma + 2b')^{1/2} + (\sigma - 2b')^{1/2}\right] - \right. \\ & \left. \frac{2(1 - \nu')}{2 - \nu'}(1 - 2b')^{1/2} + \frac{2(1 + \nu')}{2 + \nu'}(1 + 2b')^{1/2} - \frac{4\nu'}{(4 - \nu'^2)}\right\} \end{aligned}\right\} \quad (62)$$

Here $b = c = 0$. All the rest remain the same as shown in equation (59).

(d) When $\beta_0 = -1$, A and D become

$$\left.\begin{aligned} & A = B \text{ in equation (61), where } \beta_1 = 1 \\ & D = E \text{ in equation (61)} \end{aligned}\right\} \quad (63)$$

Here $a = 0$. The rest of the terms in equation (59) remain the same. This case occurs when the left characteristic coincides with the leading edge on the right side. This conforms with the reversed-flow theorem, $\beta_0 = -1 \longrightarrow \beta_1 = 1$, if the flow direction is reversed.

(e) When $\beta_1 = -1$, B and E become

$$\left.\begin{aligned} & B = A \text{ in equation (60), where } \beta_0 = 1 \\ & E = D \text{ in equation (60)} \end{aligned}\right\} \quad (64)$$

Here $a = b = c = 0$. The rest of the terms remain the same as given in equation (59).

(f) When $\beta = -1$, C and F are the same as given above for $\beta = 1$ with some rearrangement of terms and $a = c = 0$.

(g) When $\nu' = 0$, or there is no taper, $\beta_o = \beta_1 = \beta$ and equation (59) becomes

$$
\begin{aligned}
\pi b' \frac{C_D}{C_{D_o}} = (b')^2 &\left[\frac{-3\beta}{(\beta^2-1)^{1/2}} \cosh^{-1}\left|\frac{\beta^2+1}{2\beta}\right| - \cosh^{-1}\left|\frac{1}{b'}\right| + 4\cosh^{-1}\left|\frac{1}{2b'}\right|\right] + \\
&\left\{\frac{(1+\beta b')^2}{2\beta(1-\beta^2)^{1/2}}\left\{-\sin^{-1}\frac{\beta+b'}{1+\beta b'} + \sin^{-1}\left[\beta + \frac{(1-\beta^2)b'}{2(1+\beta b')}\right]\right\} + \frac{(1+2\beta b')^2}{2\beta(1-\beta^2)^{1/2}}\left\{\sin^{-1}\frac{\beta+2b'}{1+2\beta b'} - \sin^{-1}\left[\beta + \frac{(1-\beta^2)b'}{1+2\beta b'}\right]\right\}\right. \\
&\left.\frac{(1+\beta b')^2}{2\beta(\beta^2-1)^{1/2}}\left[\cosh^{-1}\left|\frac{\beta+b'}{1+\beta b'}\right| - \cosh^{-1}\left|\beta + \frac{(1-\beta^2)b'}{2(1+\beta b')}\right|\right] + \frac{(1+2\beta b')^2}{2\beta(\beta^2-1)^{1/2}}\left[-\cosh^{-1}\left|\frac{\beta+2b'}{1+2\beta b'}\right| + \cosh^{-1}\left|\beta + \frac{(1-\beta^2)b'}{1+2\beta b'}\right|\right]\right\} + \\
&\left\{\frac{(1-\beta b')^2}{2\beta(1-\beta^2)^{1/2}}\left\{-\sin^{-1}\frac{\beta-b'}{1-\beta b'} + \sin^{-1}\left[\beta - \frac{(1-\beta^2)b'}{2(1-\beta b')}\right]\right\} + \frac{(1-2\beta b')^2}{2\beta(1-\beta^2)^{1/2}}\left\{\sin^{-1}\frac{\beta-2b'}{1-2\beta b'} - \sin^{-1}\left[\beta - \frac{(1-\beta^2)b'}{1-2\beta b'}\right]\right\}\right. \\
&\left.\frac{(1-\beta b')^2}{2\beta(\beta^2-1)^{1/2}}\left[\cosh^{-1}\left|\frac{\beta-b'}{1-\beta b'}\right| - \cosh^{-1}\left|\beta - \frac{(1-\beta^2)b'}{2(1-\beta b')}\right|\right] + \frac{(1-2\beta b')^2}{2\beta(\beta^2-1)^{1/2}}\left[-\cosh^{-1}\left|\frac{\beta-2b'}{1-2\beta b'}\right| + \cosh^{-1}\left|\beta - \frac{(1-\beta^2)b'}{1+2\beta b'}\right|\right]\right\} + \\
&\left\{\frac{1}{2\beta(1-\beta^2)^{1/2}}\left\{\sin^{-1}\left[\beta + \frac{(1-\beta^2)b'}{2}\right] - \sin^{-1}\left[\beta + (1-\beta^2)b'\right] + \sin^{-1}\left[\beta - \frac{(1-\beta^2)b'}{2}\right] - \sin^{-1}\left[\beta - (1-\beta^2)b'\right]\right\}\right. \\
&\left.\frac{1}{2\beta(\beta^2-1)^{1/2}}\left[-\cosh^{-1}\left|\beta + \frac{(1-\beta^2)b'}{2}\right| + \cosh^{-1}\left|\beta + (1-\beta^2)b'\right| - \cosh^{-1}\left|\beta - \frac{(1-\beta^2)b'}{2}\right| + \cosh^{-1}\left|\beta - (1-\beta^2)b'\right|\right]\right\} + \\
&\left\{\frac{b'}{(1-\beta^2)^{1/2}}\left\{\sin^{-1}\left[\beta - \frac{(1-\beta^2)b'}{2}\right] - \sin^{-1}\left[\beta + \frac{(1-\beta^2)b'}{2}\right] + 2\sin^{-1}\left[\beta + (1-\beta^2)^{1/2}b'\right] - 2\sin^{-1}\left[\beta - (1-\beta^2)^{1/2}b'\right]\right\}\right. \\
&\left.\frac{b'}{(\beta^2-1)^{1/2}}\left[-\cosh^{-1}\left|\beta - \frac{(1-\beta^2)b'}{2}\right| + \cosh^{-1}\left|\beta + \frac{(1-\beta^2)b'}{2}\right| - 2\cosh^{-1}\left|\beta + (1-\beta^2)^{1/2}b'\right| + 2\cosh^{-1}\left|\beta - (1-\beta^2)^{1/2}b'\right|\right]\right\} + \\
&\left\{\frac{1}{(1-\beta^2)^{1/2}}\left\{-\left[\frac{4}{(2+\beta b')^2-(b')^2}\right]^{1/2} - \left[\frac{4}{(2-\beta b')^2-(b')^2}\right]^{1/2} + \left[\frac{1}{(1+\beta b')^2-(b')^2}\right]^{1/2} + \left[\frac{1}{(1-\beta b')^2-(b')^2}\right]^{1/2}\right\}\right. \\
&\left.\frac{1}{(\beta^2-1)^{1/2}}\left\{\left[\frac{4}{(2+\beta b')^2-(b')^2}\right]^{1/2} + \left[\frac{4}{(2-\beta b')^2-(b')^2}\right]^{1/2} - \left[\frac{1}{(1+\beta b')^2-(b')^2}\right]^{1/2} - \left[\frac{1}{(1-\beta b')^2-(b')^2}\right]^{1/2}\right\}\right. \qquad (65)
\end{aligned}
$$

The above equation is in accord with the results given in reference 2.

(h) If $M \longrightarrow 1$, $\beta \longrightarrow \pm\infty$ as Λ is positive or negative. By definition, $\mu = b/a_o$, $\nu' b' = \nu\mu$, $\omega = \mu \tan \Lambda$, $\omega_o = \mu \tan \Lambda_o$, and $\omega_1 = \mu \tan \Lambda_1$.

$$\frac{\pi C_D}{8a^2}\left(\frac{2}{\sigma} - \nu\right) = 3 \log \frac{1 - \nu\mu}{\omega} + \frac{1}{2} \log \frac{\omega}{\omega_o} + \frac{1}{2} \log \frac{\omega}{\omega_1} - \log 2 +$$

$$\frac{\omega}{\omega_o}\left(\frac{1}{\omega} + 1\right)^2\left[\log 2 \left(\frac{1 - \nu\mu}{1 + \omega}\right) - \log \left(\frac{2 + 2\omega - \omega_o}{1 + \omega}\right)\right] + \frac{1}{2}\left(\frac{\omega_o}{\omega + \omega_o}\right)\left(\frac{1 + \omega + \omega_o}{\omega_o}\right)^2\left(-\log \frac{1 - \nu\mu}{1 + \omega + \omega_o} + \log \frac{1 + \omega}{1 + \omega + \omega_o}\right) +$$

$$\frac{1}{2}\left(\frac{\omega}{\omega + \omega_1}\right)\left(\frac{1 + \omega + \omega_1}{\omega}\right)^2\left(-\log \frac{1 - \nu\mu}{1 + \omega + \omega_1} + \log \frac{1 + \omega_1}{1 + \omega + \omega_1}\right) + \frac{1}{2} \frac{\omega}{\omega_1}\left(\frac{1}{\omega} - 1\right)^2\left(\log \frac{1 - \nu\mu}{1 - \omega} - \log \left|1 - \frac{\omega_1}{2(1 - \omega)}\right|\right) +$$

$$\frac{1}{2}\left(\frac{\omega}{\omega + \omega_o}\right)\left(\frac{1 - \omega - \omega_o}{\omega}\right)^2\left(-\log \frac{1 - \nu\mu}{1 - \omega - \omega_o} + \log \frac{1 - \omega_o}{1 - \omega - \omega_o}\right) + \frac{1}{2} \frac{\omega_1}{\omega + \omega_1}\left(\frac{1 - \omega - \omega_1}{\omega_1}\right)^2\left(-\log \frac{1 - \nu\mu}{1 - \omega - \omega_1} + \log \frac{1 - \omega}{1 - \omega - \omega_1}\right) +$$

$$\frac{(1 - \nu\mu)^2}{2\nu\mu\omega_o}\left\{\log \left[1 + \frac{\omega_o}{2(1 - \nu\mu)}\right] - \log \left(1 + \frac{\omega_o}{1 - \nu\mu}\right)\right\} + \frac{(1 - \nu\mu)^2}{2\nu\mu\omega}\left[-\log \left(1 + \frac{\omega}{1 - \nu\mu}\right) + \log \left(1 - \frac{\omega}{1 - \nu\mu}\right)\right] +$$

$$\frac{(1 - \nu\mu)^2}{2\nu\mu\omega_1}\left\{-\log \left[1 - \frac{\omega_1}{2(1 - \nu\mu)}\right] + \log \left(1 - \frac{\omega_1}{1 - \nu\mu}\right)\right\} + \frac{1}{2\nu\mu\omega_o}\left[\left(1 - \frac{\nu\mu}{\omega}\right) \log \left(\frac{2 - \omega_o}{2}\right) - \left(\frac{\omega + \omega_o - 2\nu\mu}{\omega + \omega_o}\right) \log \left(1 - \omega_o\right)\right] +$$

$$\frac{1}{2\nu\mu\omega}\left[-\left(\frac{\omega + \omega_1 - \nu\mu}{\omega + \omega_1}\right) \log (1 - \omega) + \left(\frac{\omega + \omega_o + \nu\mu}{\omega + \omega_o}\right) \log (1 + \omega) - \frac{4\nu\mu\omega}{(\omega + \omega_1)(\omega + \omega_o)}\right] +$$

$$\frac{1}{2\nu\mu\omega_1}\left[-\left(\frac{\omega + \nu\mu}{\omega}\right) \log \left(\frac{2 + \omega_1}{2}\right) + \left(\frac{\omega + \omega_1 + \nu\mu}{\omega + \omega_1}\right) \log \left(1 + \omega_1\right) + \frac{\nu\mu\omega_1}{\omega(\omega + \omega_1)}\right] - \frac{1}{2}\left[\frac{1}{\omega(\omega + \omega_o)}\right] \tag{66}$$

There are a number of other limiting cases such as $\beta_o + \beta = 0$ $(\Lambda_o = -\Lambda)$ and $\beta_1 + \beta = 0$ $(\Lambda_1 = -\Lambda)$ which are also required in calculation. If $\sigma = 0$ and $\beta_1 = 0$, equation (59) will give the wave drag of the triangular wing which checks with Puckett's results. Owing to limited space, they are all omitted.

AERODYNAMIC BEHAVIOR OF A WING WITH A GIVEN LIFT DISTRIBUTION

From the section Supersonic Flow about a Lifting Surface,

$$g(\lambda,y) = \frac{1}{2\pi}\int_{-\infty}^{\infty} dt\ e^{-i\lambda t}C_p(t,y,+0) \tag{30}$$

Thus, when the pressure-coefficient distribution $C_p(t,y,+0)$ is given on the wing plan form, $g(\lambda,y)$ can be obtained with this equation.

Consider a tapered sweptback wing with a constant lift distribution

$$C_p(t,y) = C_{po}$$

$$-b \leqq y \leqq b$$

$$\beta_o|y| - a_o' \leqq t \leqq \beta_1|y|a_o'$$

where β_o and β_1 are defined in figure 1. Thus, at any y within the span,

$$g(\lambda,y) = \frac{1}{2\pi}\int_{\beta_o|y|-a_o'}^{\beta_1|y|a_o'} C_{po}e^{-i\lambda t}\,dt$$

$$= \frac{iC_{po}}{2\pi\lambda}\left[e^{-i\lambda\left(\beta_1|y|a_o'\right)} - e^{-i\lambda\left(\beta_o|y|-a_o'\right)}\right] \tag{67}$$

As $\lambda \rightarrow 0$, $g(0,y)$ can be evaluated as

$$g(0,y) = \frac{C_{po}}{\pi}\left(a_o' - \frac{\beta_o - \beta_1}{2}|y|\right) \tag{68}$$

Substituting the above equation in equation (24), there results

$$w(t,y,+0) = \frac{-m'U}{2}\int_{-b}^{b}\frac{d\eta}{(y-\eta)^2}\left\{\frac{C_{po}}{\pi}\left(a_o' - \frac{\beta_o - \beta_1}{2}|\eta|\right) + \right.$$

$$\left.\frac{|y-\eta|}{2}\int_{-\infty}^{\infty}d\lambda\,\frac{C_{po}}{2\pi\lambda i}\left[e^{-i\lambda(\beta_1|y|+a_o')} - \right.\right.$$

$$\left.\left.e^{-i\lambda(\beta_o|y|-a_o')}\right]e^{i\lambda t}H_1^{(2)}(\lambda|y-\eta|)\right\}$$

$$= \frac{-m'UC_{po}}{2\pi}\int_{-b}^{b}\frac{d\eta}{(y-\eta)^2}\left\{\left(a_o' - \frac{\beta_o - \beta_1}{2}|\eta|\right) - \right.$$

$$\left.\frac{i|y-\eta|}{4}\int_{-\infty}^{\infty}\frac{d\lambda}{\lambda}\left[e^{-i\lambda(\beta_1|y|+a_o')} - \right.\right.$$

$$\left.\left.e^{-i\lambda(\beta_o|y|-a_o')}\right]e^{i\lambda t}H_1^{(2)}(\lambda|y-\eta|)\right\} \tag{69}$$

With the aid of appendix C, the infinite integrals can be evaluated and

$$w(t,y,+0) = \frac{-C_{po}m'U}{2\pi}\int_{-b}^{b}\frac{d\eta}{(y-\eta)^2}\left[\left(a_o' - \frac{\beta_o - \beta_1}{2}|\eta|\right) - \right.$$

$$\frac{|y-\eta|}{2}\begin{cases} -\dfrac{t_1 - \beta_1|\eta|}{|y-\eta|} + 0, & t_1 - \beta_1|\eta| \leqq |y-\eta| \\ -\dfrac{t_1 - \beta_1|\eta|}{|y-\eta|} + \dfrac{2\sqrt{(t_1 - \beta_1|\eta|)^2 - (y-\eta)^2}}{|y-\eta|}, & t_1 - \beta_1|\eta| \geqq |y-\eta| \end{cases} -$$

$$\left.\frac{|y-\eta|}{2}\begin{cases} \dfrac{t_o - \beta_o|\eta|}{|y-\eta|}, & t_o - \beta_o|\eta| \leqq |y-\eta| \\ \dfrac{t_o - \beta_o|\eta|}{|y-\eta|} - \dfrac{2\sqrt{(t_o - \beta_o|\eta|)^2 - (y-\eta)^2}}{|y-\eta|}, & t_o - \beta_o|\eta| \geqq |y-\eta| \end{cases}\right] \tag{70}$$

where $t_o = t + a_o'$, $t_1 = t - a_o'$. Only one of the two expressions holds for the range specified in the bracket.

If the integration of η is written from 0 to b only,

$$w(t,y,+0) = \frac{-C_{po}m'U}{4\pi}\int_0^b d\eta \left\{ \frac{2a_o' - (\beta_o - \beta_1)\eta}{(y-\eta)^2} + \frac{2a_o' - (\beta_o - \beta_1)\eta}{(y+\eta)^2} - \right.$$

$$\left[\frac{2a_o' - (\beta_o - \beta_1)\eta}{(y-\eta)^2} + \frac{2a_o' - (\beta_o - \beta_1)\eta}{(y+\eta)^2} - \right.$$

$$\frac{2\sqrt{(t_o - \beta_o\eta)^2 - (y-\eta)^2}}{(y-\eta)^2} - \frac{2\sqrt{(t_o - \beta_o\eta)^2 - (y+\eta)^2}}{(y+\eta)^2} +$$

$$\left. \left. \frac{2\sqrt{(t_1 - \beta_1\eta)^2 - (y-\eta)^2}}{(y-\eta)^2} + \frac{2\sqrt{(t_1 - \beta_1\eta)^2 - (y+\eta)^2}}{(y+\eta)^2} \right] \right\}$$

$$= \frac{-C_{po}m'U}{2\pi}\int_0^b \left[\frac{\sqrt{(t_o - \beta_o\eta)^2 - (y-\eta)^2}}{(y-\eta)^2} - \right.$$

$$\frac{\sqrt{(t_1 - \beta_1\eta)^2 - (y-\eta)^2}}{(y-\eta)^2} + \frac{\sqrt{(t_o - \beta_o\eta)^2 - (y+\eta)^2}}{(y+\eta)^2} -$$

$$\left. \frac{\sqrt{(t_1 - \beta_1\eta)^2 - (y+\eta)^2}}{(y+\eta)^2} \right] \qquad (71)$$

where $t_o - t_1 = 2a_o'$ is used so that the first terms cancel out.

Now, carrying out the integration with respect to η,

$$w(t,y,+0) = \frac{C_{po}m'U}{2\pi}\left[-(A - B) + (C - D)\right] \tag{72}$$

where

$$A = \int_0^b d\eta \, \frac{\sqrt{(t_o - \beta_o\eta)^2 - (y - \eta)^2}}{(y - \eta)^2} \quad \text{(see table I)} \tag{73}$$

$$B = \int_0^b d\eta \, \frac{\sqrt{(t_1 - \beta_1\eta)^2 - (y - \eta)^2}}{(y - \eta)^2} \quad \text{(see footnote, table I)} \tag{74}$$

$$C = \int_0^b -d\eta \, \frac{\sqrt{(t_o - \beta_o\eta)^2 - (y + \eta)^2}}{(y + \eta)^2} \quad \text{(see table II)} \tag{75}$$

$$D = \int_0^b -d\eta \, \frac{\sqrt{(t_1 - \beta_1\eta)^2 - (y + \eta)^2}}{(y + \eta)^2} \quad \text{(see footnote, table II)} \tag{76}$$

The present treatment is equivalent to considering two hypothetical wings. The first one is of constant positive lift distribution (C_{po} is an assigned constant) starting at the leading edge and extending downstream to infinity with semispan b. The second wing is of constant negative lift distribution (C_{po} is an assigned negative constant)

starting at the trailing edge and also extending downstream to infinity with semispan b. The superposition of both hypothetical wings gives the aerodynamical behavior of the actual wing.

Integral A, equation (73), gives the contribution of downwash due to the right-side area of the first hypothetical wing in the forward Mach cone of the point P(t,y). Similarly, integral C, equation (75), gives the contribution for the area on the left side.

On the other hand, integral B, equation (74), gives the contribution of the right side of the second hypothetical wing. Similarly, integral D, equation (76), gives the left-side contribution.

As far as the limits of the integrals are concerned, each holds for within the limit 0 to b, whenever the integrand is a positive real quantity. However, for many locations of P(t,y), the integrand is positive only in a much narrower range of η than the interval (0,b). In order to determine the valid range of the integrals and their respective values for all possible locations of P, tables I and II are given. The corresponding values of the integrals for the different cases are given in the right-hand columns of the tables.

Take table I as an example. If the leading edge is subsonic $(\beta_o > 1)$, the lower limit of η is always zero because the forward Mach cone at P always intersects the wing center line within the wing area. When $\beta_o > 1$ the upper limit of η is given in the upper half of table I. Condition 1 concerns the location of the point P, which may be ahead of, on, or behind the leading edge, while condition 2 concerns the right intersection of the forward Mach cone of P with the leading edge, or side edge. Under both conditions 1 and 2, there are six possible cases. The upper limit of η is given in each case, and the value of the integral A is also given accordingly.

If the leading edge is supersonic $(\beta_o < 1)$, the integral A exists only when the point P is behind the leading edge. In particular, both the upper and the lower limit may vary within the interval (0,b). The condition for the lower limit depends on the intersection of the left side of the forward Mach cone of P. It is zero when and only when the intersection is on the center line of the wing in the wing area. If the intersection is on the right-side leading edge, the lower limit is $\frac{y - t_o}{1 - \beta_o}$ as indicated. The condition for the upper limit depends on the right-hand intersection of the forward Mach cone of P. If the right side of the forward Mach cone cuts the leading edge within the span, the upper limit is $\frac{t_o + y}{1 + \beta_o}$; otherwise, the upper limit of η is b.

The tables for the other three integrals can be explained similarly. Figure 6 shows four typical cases concerning the integral limits. Figure 6(a) shows the forward Mach cone of a point $P(t,y)$ that lies only in the right-side area of the wing. Therefore only integral A exists and all the other three integrals are zero. Since the leading edge is supersonic $(\beta_o < 1)$, the upper integral limit is $\frac{t_o + y}{1 + \beta_o}$. It belongs to integral A-9 as indicated, according to table I. Figure 6(b) shows the forward Mach cone covering both the left- and right-side areas of the wing. Thus, only integrals A and C exist. The integrals are indicated. Figures 6(c) and 6(d) can be similarly explained.

Although the lift distribution of the wing with supersonic trailing edge is well-known, the downwash may be interesting to explore. Figure 7 shows three infinite half-wings with trailing edges at 15°, 30°, and 45° from the leading edge which is normal to the direction of flight. This is shown in the t,y-plane, or the x,y-plane with a Mach number equal to $\sqrt{2}$. A negative infinite downwash always occurs at the tip. The curves are plotted as $2\pi w(y/t)/m'C_{po}U$ against y/t. As is known, $C_{po} = 2\alpha_1/m'$, where α_1 is the angle of attack of the wing; therefore, $\pi w/\alpha_1 U$ can be plotted against y/t. Between the tip cone and the wing the downwash is constant but increases with increasing trailing-edge angle. Owing to the conical flow, the downwash is identically the same along the radial lines expressed in the conical coordinate y/t. The above curves were calculated with equation (72) and the tables for integrals A and B by setting $\beta_o = 0$; $\beta_1 = \tan 15°$, $\tan 30°$, and $\tan 45°$; and $a_o' = 0$. (Here $t = t_o = t_1$.)

Figure 8 shows a wing tip of unit chord with a raked angle of 30° for three values of t. At $t = 0.5$, it behaves exactly the same as the 30° case of figure 7(b), but at $t = 1.5$, it is quite different. Two infinite downwashes occur, one at the center of the leading-edge tip cone, and the other at the center of the trailing-edge tip cone. The former remains negative, the latter positive. Outside the two tip Mach cones, the downwash is identically zero as predicted by the two-dimensional theory. The above calculations can be made from equation (72) and the tables for integrals A, B, and C by letting $\beta_o = \beta_1 = \tan 30°$ and $a_o' = 0.5$. (Here $t = t_o - 0.5 = t_1 + 0.5$.)

As another interesting example, the downwash distribution near the nose of an infinite constant-chord sweptback wing is calculated (fig. 9). The leading edge is swept back at 30° but is still supersonic. The downwash at different locations on the span is plotted along t. In

this case, the curves are plotted with $\frac{\sqrt{1-\beta_o^2}}{\alpha_1}\frac{w(t,y)}{U}$ against t at different values of y where $C_{po} = \frac{2\alpha_1}{m'\sqrt{1-\beta_o^2}}$ is introduced.

At $y = 0$, the downwash angle reaches the maximum value (0.8165) at a single nose point and remains zero along the chord up to the trailing edge. There the downwash angle is negative and equal to the maximum value in magnitude and recovers to zero downwash downstream. For instance, at $y = 0.4$, the downwash angle is constant in the supersonic region, and drops down under the influence of the nose Mach cone. At the trailing edge, the downwash angle drops to a negative value abruptly and continues to decrease until the trailing Mach cone is reached. The drop of downwash at the trailing edge is exactly equal to the downwash angle at the supersonic leading edge. Further along t, the downwash angle rises again and becomes asymptotic to 0 as $t \rightarrow \infty$. The same can be applied at any value of y until the nose Mach cone is off the trailing edge.

Of course, it is very difficult to build a wing with the angle of attack as required by the constant pressure distribution. But by the present method it is so simple to calculate the downwash distribution anywhere in the plane of the wing that it will surely afford many applications if the trailing edge is supersonic. With a given pressure distribution, it is easy to calculate the sidewash; however, the details are omitted here.

As another example, the downwash of a finite triangular wing with a 60° sweptback angle is calculated. Figure 10 shows the downwash distributions at different values of y. Figure 11 shows the downwash distribution of a tapered sweptback wing. The taper ratio is 1/6. Figure 12 shows the downwash of the same sweptback wing far downstream. It is very interesting to examine the effect of different Mach cones on the downwash. One important feature of the subsonic leading edge is the infinite downwash angle. As before, the above curves are calculated with equation (72) and the tables for integrals A, B, C, and D.

The present approach to calculating downwash of a wing with constant lift distribution cannot be applied to wings with subsonic trailing edges, because the Joukowski-Kutta condition must be satisfied at such trailing edges. In order to investigate the case with a subsonic trailing edge, it is necessary to assume the distribution of the pressure coefficient drops to zero at the trailing edge.

The preceding discussion just gives some cases with simple pressure distribution along the chord to demonstrate the application of the method. Of course the method is not limited to these cases alone.

The Johns Hopkins University
Baltimore, Md., November 4, 1949

APPENDIX A

FOURIER TRANSFORM OF THE SLOPE DISTRIBUTION ON AN AIRFOIL

As an example of the slope distribution on an airfoil, the Fourier transform of the slope on a double-wedge airfoil is calculated.

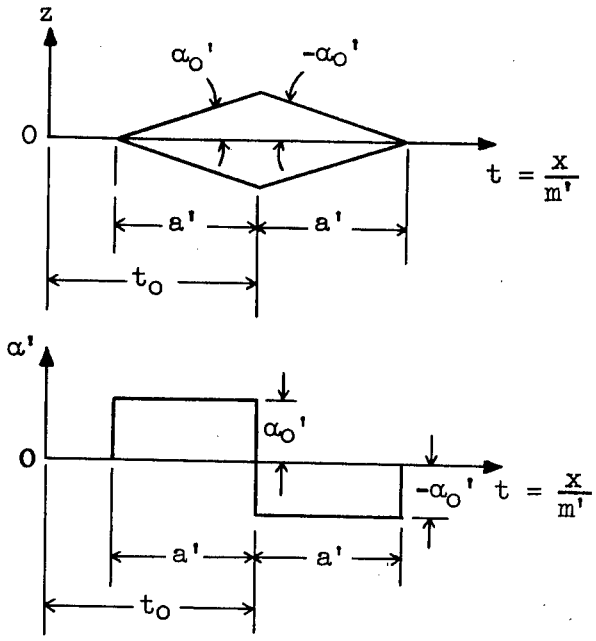

The accompanying figure shows the shape and slope of a double-wedge airfoil on a sweptback wing at a distance y from the center of the wing span. The slope distribution is as follows:

$$\left.\begin{aligned} \alpha(t,y) &= 0, \quad t < t_o(y) - a'(y) \\ \alpha(t,y) &= \alpha_o'(y), \quad t_o(y) - a'(y) < t \leqq t_o \\ \alpha(t,y) &= -\alpha_o'(y), \quad t_o \leqq t < t_o(y) + a'(y) \\ \alpha(t,y) &= 0, \quad t > t_o(y) + a'(y) \end{aligned}\right\} \tag{A1}$$

where α, α_o', t_o and a' are functions of y in general. Substituting equation (A1) into equation (19), it yields

$$f(\lambda,y) = f_0(\lambda,y) + if_1(\lambda,y)$$

$$= \frac{1}{2\pi}\int_{-\infty}^{\infty} \alpha(t,y)e^{-i\lambda t}\,dt$$

$$= \frac{\alpha_o'}{2\pi}\int_{t_o-a'}^{t_o} e^{-i\lambda t}\,dt - \frac{\alpha_o'}{2\pi}\int_{t_o}^{t_o+a'} e^{-i\lambda t}\,dt$$

$$= \frac{\alpha_o}{2\pi}e^{-i\lambda t_o}\left(\int_{-a'}^{0} e^{-i\lambda\tau}\,d\tau - \int_{0}^{a'} e^{-i\lambda\tau}\,d\tau\right) \qquad (A2)$$

where $t = t_o + \tau$ is used in substitution. It is easy to show that

$$f(\lambda,y) = \frac{-\alpha_o'}{i\pi\lambda}e^{-i\lambda t_o}(1 - \cos\lambda a') \qquad (A3)$$

$$f_0(\lambda,y) = \frac{\alpha_o'}{\pi\lambda}\sin\lambda t_o(1 - \cos\lambda a') \quad \text{(even with respect to } \lambda) \qquad (A4)$$

$$f_1(\lambda,y) = \frac{\alpha_o'}{\pi\lambda}\cos\lambda t_o(1 - \cos\lambda a') \quad \text{(odd with respect to } \lambda) \qquad (A5)$$

For a rectangular wing with constant airfoil section, where α_o', t_o, and a' are independent of y in the span, equations (A4) and (A5) reduce to

$$f_0(\lambda,y) = 0$$

$$f_1(\lambda,y) = \frac{\alpha_o'}{\pi\lambda}(1 - \cos \lambda a')$$

if t_o is chosen equal to zero.

For the case of a straight tapered sweptback wing, as shown in figure 1,

$$a'(y) = \frac{a_o - \nu|y|}{m'}$$

$$t_o(y) = \beta|y|$$

$$\alpha_o'(y) = \alpha_o' \quad \text{independent of} \quad y$$

For the details of the definitions of the different parameters, refer to the figure. Then,

$$\left.\begin{aligned} f_0(\lambda,y) &= \frac{\alpha_o'}{\pi\lambda} \sin(\lambda\beta|y|)(1 - \cos \lambda a_y') \\ f_1(\lambda,y) &= \frac{\alpha_o'}{\pi\lambda} \cos(\lambda\beta|y|)(1 - \cos \lambda a_y') \end{aligned}\right\} \quad (A6)$$

Now,

$$f(\lambda,y)\overline{f(\lambda,\eta)} = \left[\frac{-\alpha_o'}{i\pi\lambda} e^{-i\lambda\beta|y|}\left(1 - \cos \lambda a_y'\right)\right]\left[\frac{\alpha_o'}{i\pi\lambda} e^{-i\lambda\beta|\eta|}\left(1 - \cos \lambda a_y'\right)\right]$$

$$= \frac{\alpha_o^2}{\pi^2\lambda^2} e^{-i\lambda\beta(|y| - |\eta|)}\left(1 - \cos \lambda a_y'\right)\left(1 - \cos \lambda a_\eta'\right)$$

$$= \frac{(\alpha_o')^2}{\pi^2\lambda^2}\left(1 - \cos \lambda a_y'\right)\left(1 - \cos \lambda a_\eta'\right)\left[\cos \lambda\beta(|y| - |\eta|) - i \sin \lambda\beta(|y| - |\eta|)\right]$$

$$= \left[f_0(\lambda,y)f_0(\lambda,\eta) + f_1(\lambda,y)f_1(\lambda,\eta)\right] + i\left[f_1(\lambda,y)f_0(\lambda,\eta) - f_0(\lambda,y)f_1(\lambda,\eta)\right] \tag{A7}$$

Therefore, separating the real and imaginary parts,

$$f_0(\lambda,y)f_0(\lambda,\eta) + f_1(\lambda,y)f_1(\lambda,\eta) = \frac{(\alpha_o')^2}{\pi^2\lambda^2}\left(1 - \cos \lambda a_y'\right)\left(1 - \cos \lambda a_\eta'\right) \cos \lambda\beta(|y| - |\eta|) \tag{A8}$$

$$-f_1(\lambda,y)f_0(\lambda,\eta) + f_0(\lambda,y)f_1(\lambda,\eta) = \frac{(\alpha_o')^2}{\pi^2\lambda^2}\left(1 - \cos \lambda a_y'\right)\left(1 - \cos \lambda a_\eta'\right) \sin \lambda\beta(|y| - |\eta|) \tag{A9}$$

APPENDIX B

SYMBOLS

a velocity of sound

a_o half root chord

$a_o' = a_o/m'$

a_t half tip chord

$a_t' = a_t/m'$

a_y half chord at y $\left(a_o - \nu|y|\right)$

$a_y' = a_y/m'$

A aspect ratio $\left(\frac{2b}{a_o + a_t}\right)$

b half span

$b' = \frac{b}{a_o'} = \frac{1 + \sigma}{2\beta} A \tan \Lambda$

C_D wave drag coefficient

C_{Do} two-dimensional wave drag coefficient $\left(4a_o^2/m'\right)$

C_L lift coefficient

C_p pressure coefficient

C_{po} two-dimensional pressure coefficient or assigned pressure coefficient

D drag

$F(\lambda,\eta)$ distribution function of the harmonic source (complex); see equation (5)

$f(\lambda,\eta) = -\frac{1}{4} F(\lambda,\eta)$

$G(\lambda,\eta)$ doublet distribution function (complex); see equation (7)

$g(\lambda,\eta) = \frac{i\lambda G(\lambda,\eta)}{8m'}$

$H_0^{(1)}(\ )$ Hankel function of the first kind of zero order

$H_0^{(2)}(\ )$ Hankel function of the second kind of zero order

$H_1^{(1)}(\ )$ Hankel function of the first kind of first order

$H_1^{(2)}(\ )$ Hankel function of the second kind of first order

$\overline{H_1^{(2)}(\ )}$ conjugate of $H_1^{(2)}(\ )$ $\left(J_1(\ ) + iY_1(\ )\right)$

$J_0(\ )$ Bessel function of zero order

$J_1(\ )$ Bessel function of first order

M Mach number

$m' = \sqrt{M^2 - 1}$

$\bar{n}$ unit vector normal to solid surface

p pressure

p_o free-stream static pressure

$\bar{q}$ velocity vector

$r = \sqrt{(y - \eta)^2 + z^2}$

t longitudinal coordinate in transformed plane (equivalent to time in supersonic case) (x/m')

$t_o = t + a_o'$

$t_1 = t - a_o'$

U free-stream velocity

u velocity component in x- (or t-) direction

v velocity component in y-direction

w velocity component in z-direction

x longitudinal axis

y spanwise axis

$y' = y/a_o'$

$Y_0(\ )$ Bessel function of the second kind of zero order

$Y_1(\ )$ Bessel function of the second kind of first order

z vertical axis

α angle of attack

α_+ angle of attack of upper surface of airfoil

α_- angle of attack of lower surface of airfoil

α_o slope of upper surface on symmetrical airfoil

α_1 angle of attack of cambered wing

$\beta = \dfrac{\tan \Lambda}{m'} = \tan \Lambda'$

$\beta_o = \beta + \nu'$

$\beta_1 = \beta - \nu'$

Λ angle between midchord and y-axis (x,y-plane)

Λ' angle between midchord and y-axis (t,y-plane)

Λ_o leading-edge sweepback angle (x,y-plane)

Λ_1 trailing-edge sweepback angle (x,y-plane)

ζ source location along z-axis

η source location along y-axis

$\theta = \tan^{-1} \frac{\eta - y}{z}$

λ oscillation frequency of continuous spectrum

$\mu = b/a_o$

$\nu = \frac{a_o - a_t}{b}$

$\nu' = \frac{\nu}{m'} = \frac{1 - \sigma}{b'}$

ξ source location along x-axis (t-axis)

ρ density

ρ_o free-stream density

σ taper ratio $\left(a_t/a_o\right)$

$\tau = \xi/m'$

ϕ velocity potential

χ^* potential in Trefftz plane

$\omega = \mu \tan \Lambda$

$\omega_o = \mu \tan \Lambda_o$

$\omega_1 = \mu \tan \Lambda_1$

APPENDIX C

INTEGRALS FOR USE IN TEXT

The following integrals are those which are used often in the text and many of which are not available in the ordinary handbook. In the first 13 formulas, the upper line corresponds to $\beta < 1$, and the lower line to $\beta > 1$.

$$\int du \sin^{-1}\left(\frac{K}{u} \mp \beta\right) = u \sin^{-1}\left(\frac{K}{u} \mp \beta\right) + \begin{cases} \dfrac{\pm K}{(1-\beta^2)^{1/2}} \cosh^{-1}\left[\beta \pm (1-\beta)^2 \dfrac{u}{K}\right] \\ \dfrac{\mp K}{(\beta^2-1)^{1/2}} \sin^{-1}\left[\beta \mp (\beta^2-1)\dfrac{u}{K}\right] \end{cases}$$

$$\int du \sin^{-1}\left(\beta \mp \frac{K}{u}\right) = u \sin^{-1}\left(\beta \mp \frac{K}{u}\right) + \begin{cases} \dfrac{\mp K}{(1-\beta^2)^{1/2}} \cosh^{-1}\left[(1-\beta^2)\dfrac{u}{K} \pm \beta\right] \\ \dfrac{\mp K}{(\beta^2-1)^{1/2}} \sin^{-1}\left[(\beta^2-1)\dfrac{u}{K} \mp \beta\right] \end{cases}$$

$$\int du \cosh^{-1}\left(\frac{K}{u} \mp \beta\right) = u \cosh^{-1}\left(\frac{K}{u} \mp \beta\right) + \begin{cases} \dfrac{\pm K}{(1-\beta^2)^{1/2}} \sin^{-1}\left[\beta \pm (1-\beta^2)\dfrac{u}{K}\right] \\ \dfrac{\mp K}{(\beta^2-1)^{1/2}} \cosh^{-1}\left[\beta \mp (\beta^2-1)\dfrac{u}{K}\right] \end{cases}$$

$$\int du \cosh^{-1}\left(\beta \mp \frac{K}{u}\right) = u \cosh^{-1}\left(\beta \mp \frac{K}{u}\right) + \begin{cases} \dfrac{\mp K}{(1-\beta^2)^{1/2}} \sin^{-1}\left[(1-\beta^2)\dfrac{u}{K} \pm \beta\right] \\ \dfrac{\mp K}{(\beta^2-1)^{1/2}} \cosh^{-1}\left[(\beta^2-1)\dfrac{u}{K} \mp \beta\right] \end{cases}$$

$$\int u\,du\,\sin^{-1}\left(\frac{K}{u} \mp \beta\right) = \frac{u^2}{2}\sin^{-1}\left(\frac{K}{u} \mp \beta\right) + \begin{cases} \dfrac{K^2}{2(1-\beta^2)^{3/2}}\left\{-\beta\cosh^{-1}\left[\beta \pm (1-\beta^2)\frac{u}{K}\right] + \sqrt{\left[\beta \pm (1-\beta^2)\frac{u}{K}\right]^2 - 1}\right\} \\ \dfrac{K^2}{2(\beta^2-1)^{3/2}}\left\{-\beta\sin^{-1}\left[\beta \mp (\beta^2-1)\frac{u}{K}\right] - \sqrt{1-\left[\beta \mp (\beta^2-1)\frac{u}{K}\right]^2}\right\} \end{cases}$$

$$\int u\,du\,\sin^{-1}\left(\beta \mp \frac{K}{u}\right) = \frac{u^2}{2}\sin^{-1}\left(\beta \mp \frac{K}{u}\right) + \begin{cases} \dfrac{K^2}{2(1-\beta^2)^{3/2}}\left\{\beta\cosh^{-1}\left[(1-\beta^2)\frac{u}{K} \pm \beta\right] \mp \sqrt{\left[(1-\beta^2)\frac{u}{K} \pm \beta\right]^2 - 1}\right\} \\ \dfrac{K^2}{2(\beta^2-1)^{3/2}}\left\{-\beta\sin^{-1}\left[(\beta^2-1)\frac{u}{K} \mp \beta\right] \pm \sqrt{1-\left[(\beta^2-1)\frac{u}{K} - \beta\right]^2}\right\} \end{cases}$$

$$\int u\,du\,\cosh^{-1}\left(\frac{K}{u} \mp \beta\right) = \frac{u^2}{2}\cosh^{-1}\left(\frac{K}{u} \mp \beta\right) + \begin{cases} \dfrac{K^2}{2(1-\beta^2)^{3/2}}\left\{-\beta\sin^{-1}\left[\beta \pm (1-\beta^2)\frac{u}{K}\right] - \sqrt{1-\left[\beta \pm (1-\beta^2)\frac{u}{K}\right]^2}\right\} \\ \dfrac{K^2}{2(\beta^2-1)^{3/2}}\left\{-\beta\cosh^{-1}\left[\beta \mp (\beta^2-1)\frac{u}{K}\right] + \sqrt{\left[\beta \mp (1-\beta^2)\frac{u}{K}\right]^2 - 1}\right\} \end{cases}$$

$$\int u\,du\,\cosh^{-1}\left(\beta \mp \frac{K}{u}\right) = \frac{u^2}{2}\cosh^{-1}\left(\beta \mp \frac{K}{u}\right) + \begin{cases} \dfrac{K^2}{2(1-\beta^2)^{3/2}}\left\{\beta\sin^{-1}\left[(1-\beta^2)\frac{u}{K} \pm \beta\right] \pm \sqrt{1-\left[(1-\beta^2)\frac{u}{K} \pm \beta\right]^2}\right\} \\ \dfrac{K^2}{2(\beta^2-1)^{3/2}}\left\{-\beta\cosh^{-1}\left[(\beta^2-1)\frac{u}{K} \mp \beta\right] \mp \sqrt{\left[(\beta^2-1)\frac{u}{K} \mp \beta\right]^2 - 1}\right\} \end{cases}$$

$$\int du\,\sqrt{u^2 - (K \mp \beta u)^2} = \begin{cases} \dfrac{\pm K^2}{2(1-\beta^2)^{3/2}}\left\{\left[\beta \pm (1-\beta^2)\frac{u}{K}\right]\sqrt{\left[\beta \pm (1-\beta^2)\frac{u}{K}\right]^2 - 1} - \cosh^{-1}\left[\beta \pm (1-\beta^2)\frac{u}{K}\right]\right\} \\ \dfrac{\mp K^2}{2(\beta^2-1)^{3/2}}\left\{\left[\beta \mp (\beta^2-1)\frac{u}{K}\right]\sqrt{1-\left[\beta \mp (\beta^2-1)\frac{u}{K}\right]^2} + \sin^{-1}\left[\beta \mp (\beta^2-1)\frac{u}{K}\right]\right\} \end{cases}$$

$$\int du\,\sqrt{u^2 - (\beta u \mp K)^2} = \begin{cases} \dfrac{K^2}{2(1-\beta^2)^{3/2}}\left\{\left[(1-\beta^2)\frac{u}{K} \pm \beta\right]\sqrt{\left[(1-\beta^2)\frac{u}{K} \pm \beta\right]^2 - 1} - \cosh^{-1}\left[(1-\beta^2)\frac{u}{K} \pm \beta\right]\right\} \\ \dfrac{K^2}{2(\beta^2-1)^{3/2}}\left\{\left[(\beta^2-1)\frac{u}{K} \mp \beta\right]\sqrt{1-\left[(\beta^2-1)\frac{u}{K} \mp \beta\right]^2} + \sin^{-1}\left[(\beta^2-1)\frac{u}{K} \mp \beta\right]\right\} \end{cases}$$

$$\int du\sqrt{(K \mp \beta u)^2 - u^2} = \begin{cases} \dfrac{\pm K^2}{2(1-\beta^2)^{3/2}}\left\{\left[\beta \pm (1-\beta^2)\dfrac{u}{K}\right]\sqrt{1-\left[\beta \pm (1-\beta^2)\dfrac{u}{K}\right]^2} + \sin^{-1}\left[\beta \pm (1-\beta^2)\dfrac{u}{K}\right]\right\} \\ \dfrac{\mp K^2}{2(\beta^2-1)^{3/2}}\left\{\left[\beta \mp (\beta^2-1)\dfrac{u}{K}\right]\sqrt{\left[\beta \mp (\beta^2-1)\dfrac{u}{K}\right]^2 - 1} - \cosh^{-1}\left[\beta \mp (\beta^2-1)\dfrac{u}{K}\right]\right\} \end{cases}$$

$$\int du\sqrt{(\beta u \mp K)^2 - u^2} = \begin{cases} \dfrac{K^2}{2(1-\beta^2)^{3/2}}\left\{\left[(1-\beta^2)\dfrac{u}{K} \pm \beta\right]\sqrt{1-\left[(1-\beta^2)\dfrac{u}{K} \pm \beta\right]^2} + \sin^{-1}\left[(1-\beta^2)\dfrac{u}{K} \pm \beta\right]\right\} \\ \dfrac{K^2}{2(\beta^2-1)^{3/2}}\left\{\left[(\beta^2-1)\dfrac{u}{K} \mp \beta\right]\sqrt{\left[(\beta^2-1)\dfrac{u}{K} \mp \beta\right]^2 - 1} - \cosh^{-1}\left[(\beta^2-1)\dfrac{u}{K} \mp \beta\right]\right\} \end{cases}$$

$$\int u\,du\left[\left(\frac{K}{u} \mp \beta\right)\cosh^{-1}\left(\frac{K}{u} \mp \beta\right) - \sqrt{\left(\frac{K}{u} \mp \beta\right)^2 - 1}\right] =$$

$$\left(K \mp \frac{\beta u}{2}\right)u\cosh^{-1}\left(\frac{K}{u} \mp \beta\right) + \begin{cases} \dfrac{\pm K^2}{2(1-\beta^2)^{1/2}}\sin^{-1}\left[\beta \pm (1-\beta^2)\dfrac{u}{K}\right] + \dfrac{-Ku}{2(1-\beta^2)^{1/2}}\sqrt{1-\left[\beta \pm (1-\beta^2)\dfrac{u}{K}\right]^2} \\ \dfrac{\mp K^2}{2(\beta^2-1)^{1/2}}\cosh^{-1}\left[\beta \mp (\beta^2-1)\dfrac{u}{K}\right] + \dfrac{-Ku}{2(\beta^2-1)^{1/2}}\sqrt{\left[\beta \mp (\beta^2-1)\dfrac{u}{K}\right]^2 - 1} \end{cases}$$

$$\int_0^\infty \frac{J_0(at)(1-\cos bt)}{t}\,dt = \begin{cases} \sin^{-1}\dfrac{b}{a} & (a > b) \\ \cosh^{-1}\dfrac{b}{a} & (b > a) \end{cases}$$

$$\int_0^\infty \frac{dt}{t}J_1(at)\sin bt = \begin{cases} \dfrac{b}{a} & (a > b) \\ \dfrac{b - \sqrt{b^2 - a^2}}{a} & (b > a) \end{cases}$$

$$\int_0^\infty \frac{dt}{t^2}J_1(at)(1-\cos bt) = \begin{cases} \dfrac{a}{2} & (a > b) \\ \dfrac{a}{2}\cosh^{-1}\dfrac{b}{a} + \dfrac{b}{2a}\left(b - \sqrt{b^2 - a^2}\right) & (b > a) \end{cases}$$

$$\int_0^\infty \frac{dt}{t}Y_0(at)\sin bt = \begin{cases} 0 & (a > b) \\ -\cosh^{-1}\dfrac{b}{a} & (b > a) \end{cases}$$

$$\int_0^\infty \frac{dt}{t} Y_0(at)(1 - \cos bt) = \begin{cases} \frac{1}{\pi}\left(\sin^{-1}\frac{b}{a}\right)^2 & (a \geq b) \\ \frac{1}{\pi}\left\{\frac{\pi^2}{4} - \left[\cosh^{-1}\left(\frac{b}{a}\right)\right]^2\right\} & (b \geq a) \end{cases}$$

$$\int_0^\infty \frac{dt}{t} Y_1(at) \cos bt = \begin{cases} 0 & (a > b) \\ \frac{\sqrt{b^2 - a^2}}{a} & (b > a) \end{cases}$$

$$\int_0^\infty \frac{dt}{t^2} Y_1(at) \sin bt = \begin{cases} 0 & (a > b) \\ \frac{1}{2a}\left(b\sqrt{b^2 - a^2} - a^2 \cosh^{-1}\frac{b}{a}\right) & (b > a) \end{cases}$$

$$\int_0^a z^{2s}\left(a^2 - z^2\right)^{1/2} dz = \frac{(2s - 1)!a^{2s+2}}{4^s(s + 1)!(s - 1)!}\frac{\pi}{2}$$

$$\int_0^\infty \frac{dt}{t} Y_1(at)(1 - \cos bt) = \begin{cases} 0 & (a > b) \\ \frac{-\sqrt{b^2 - a^2}}{a} & (b > a) \end{cases}$$

$$\int d\eta \frac{\sqrt{(t_1 - \beta_1\eta)^2 - (y - \eta)^2}}{(y - \eta)^2} = \int \frac{\sqrt{N}}{\nu^2} d\eta = \frac{\sqrt{N}}{\nu} + \beta_1 \cosh^{-1}\frac{t_1 - \beta_1\eta}{y - \eta} + \begin{cases} \sqrt{\beta_1^2 - 1}\cosh^{-1}\frac{(\beta_1^2 - 1)\eta + y - \beta_1 t_1}{t_1 - \beta_1 y} \\ \sqrt{1 - \beta_1^2}\sin^{-1}\frac{(\beta_1^2 - 1)\eta + y - \beta_1 t_1}{t_1 - \beta_1 y} \end{cases}$$

$$\int d\eta \frac{\sqrt{(t_1 - \beta_1\eta)^2 - (y + \eta)^2}}{(y + \eta)^2} = \int \frac{\sqrt{N'}}{\nu'^2} d\eta = -\frac{\sqrt{N'}}{\nu'} - \beta_1 \cosh^{-1}\frac{t_1 - \beta_1\eta}{y + \eta} + \begin{cases} \sqrt{\beta^2 - 1}\cosh^{-1}\frac{(\beta_1^2 - 1)\eta - (y + \beta_1 t_1)}{t_1 + \beta_1 y} \\ -\sqrt{1 - \beta^2}\sin^{-1}\frac{(\beta_1^2 - 1)\eta - (y + \beta_1 t_1)}{t_1 + \beta_1 y} \end{cases}$$

In the last two formulas, use upper line if $\beta_1 > 1$, lower line if $\beta_1 < 1$. Similar integrals for β_0 are obtained by substituting t_0 for t_1, β_0 for β_1.

REFERENCES

1. Von Kármán, Theodor: Neue Darstellung der Tragflügeltheorie. Z.f.a.M.M., Bd. 15, Heft 1/2, Feb. 1935, pp. 56-61.

2. Von Kármán, Theodore: Supersonic Aerodynamics - Principles and Applications. Jour. Aero. Sci., vol. 14, no. 7, July 1947, pp. 373-402.

3. Busemann, A.: Infinitesimale kegelige Überschallströmung. Sonderdruck, Jahr. 1942/43 der deutschen Akademie der Luftfahrtforschung, Bd. 7B, Nr. 3, pp. 105-122, 1943. (Available in translation as NACA TM 1100, 1947.)

4. Lagerstrom, P. A.: Linearized Supersonic Theory of Conical Wings. NACA TN 1685, 1950.

5. Hayes, Wallace D.: Linearized Supersonic Flow. Ph. D. Thesis, C.I.T., 1947.

6. Stewart, H. J.: The Lift of a Delta Wing at Supersonic Speeds. Quart. Appl. Math., vol. IV, no. 3, Oct. 1946, pp. 246-254.

7. Laporte, O., and Bartels, R. C. F.: An Investigation of the Exact Solutions of the Linearized Equations for the Flow past Conical Bodies. Bumblebee Ser., Rep. No. 75, Contract NOrd 7924, Bur. Ord., U. S. Navy, and Eng. Res. Inst., Univ. of Mich., Feb. 1948.

8. Snow, Robert M.: Aerodynamics of Thin Quadrilateral Wings at Supersonic Speeds. Quart. Appl. Math., vol. V, no. 4, Jan. 1948, pp. 417-428.

9. Jones, Robert T.: Properties of Low-Aspect-Ratio Pointed Wings at Speeds below and above the Speed of Sound. NACA Rep. 835, 1946. (Formerly NACA TN 1032.)

10. Jones, Robert T.: Thin Oblique Airfoils at Supersonic Speed. NACA Rep 851, 1946. (Formerly NACA TN 1107.)

11. Puckett, Allen E.: Supersonic Wave Drag of Thin Airfoils. Jour. Aero. Sci., vol. 13, no. 9, Sept. 1946, pp. 475-484.

12. Evvard, John C.: Distribution of Wave Drag and Lift in the Vicinity of Wing Tips at Supersonic Speeds. NACA TN 1382, 1947.

13. Evvard, John C.: Theoretical Distribution of Lift on Thin Wings at Supersonic Speeds (An Extension). NACA TN 1585, 1948.

14. Heaslet, Max. A., Lomax, Harvard, and Jones, Arthur L.: Volterra's Solution of the Wave Equation as Applied to Three-Dimensional Supersonic Airfoil Problems. NACA Rep. 889, 1947. (Formerly NACA TN 1412.)

15. Heaslet, Max. A., and Lomax, Harvard: The Use of Source-Sink and Doublet Distributions Extended to the Solution of Boundary-Value Problems in Supersonic Flow. NACA Rep. 900, 1948. (Formerly NACA TN 1515.)

16. Gunn, J. C.: Linearized Supersonic Aerofoil Theory. Parts I and II. Phil. Trans. Roy. Soc. (London), ser. A, vol. 240, no. 820, Dec. 1947, pp. 327-373.

17. Lamb, Horace: Hydrodynamics. Sixth ed., Cambridge Univ. Press, 1932.

18. Watson, G. N.: A Treatise on the Theory of Bessel Functions. Second ed., The Macmillan Co., 1944.

19. Titchmarsh, E. C.: Introduction to the Theory of Fourier Integrals. The Clarendon Press (Oxford), 1937.

TABLE I

INTEGRATION LIMITS OF η AND CORRESPONDING VALUES OF THE INTEGRAL A[1]

$\beta_o > 1$ (The lower limit is always zero.)

	Condition 1	Condition 2	Upper limit	Integral A
1	$t_o > \beta_o y$	$\frac{t_o - y}{\beta_o - 1} < b$	$\frac{t_o - y}{\beta_o - 1}$	$\frac{\sqrt{t_o^2 - y^2}}{y} + \beta_o \cosh^{-1}\frac{t_o}{y} + \sqrt{\beta_o^2 - 1}\cosh^{-1}\frac{y - \beta_o t_o}{t_o - \beta_o y}$
2	$t_o > \beta_o y$	$\frac{t_o - y}{\beta_o - 1} \geqq b$	b	$\frac{\sqrt{t_o^2 - y^2}}{y} + \beta_o \cosh^{-1}\frac{t_o}{y} + \sqrt{\beta_o^2 - 1}\cosh^{-1}\frac{y - \beta_o t_o}{t_o - \beta_o y} - \frac{\sqrt{(t_o - \beta_o b)^2 - (y - b)^2}}{y - b} - \beta_o \cosh^{-1}\frac{t_o - \beta_o b}{y - b} - \sqrt{\beta_o^2 - 1}\cosh^{-1}\frac{(\beta_o^2 - 1)b + y - \beta_o t_o}{t_o - \beta_o y}$
3	$t_o = \beta_o y$	$y < b$	y	∞
4	$t_o = \beta_o y$	$y \geqq b$	b	∞
5	$t_o < \beta_o y$	$\frac{t_o + y}{\beta_o + 1} < b$	$\frac{t_o + y}{\beta_o + 1}$	$\frac{\sqrt{t_o^2 - y^2}}{y} + \beta_o \cosh^{-1}\frac{t_o}{y} + \sqrt{\beta_o^2 - 1}\cosh^{-1}\frac{y - \beta_o t_o}{t_o - \beta_o y}$
6	$t_o < \beta_o y$	$\frac{t_o + y}{\beta_o + 1} \geqq b$	b	$\frac{\sqrt{t_o^2 - y^2}}{y} + \beta_o \cosh^{-1}\frac{t_o}{y} + \sqrt{\beta_o^2 - 1}\cosh^{-1}\frac{y - \beta_o t_o}{t_o - \beta_o y} - \frac{\sqrt{(t_o - \beta_o b)^2 - (y - b)^2}}{y - b} - \beta_o \cosh^{-1}\frac{t_o - \beta_o b}{y - b} - \sqrt{\beta_o^2 - 1}\cosh^{-1}\frac{(\beta_o^2 - 1)b + y - \beta_o t_o}{t_o - \beta_o y}$

$\beta_o < 1$ (The integral exists only when $t_o > \beta_o y$.)

	Condition	Lower limit	Condition	Upper limit	Integral A
7	$\frac{y - t_o}{1 - \beta_o} \leqq 0$	0	$\frac{t_o + y}{1 + \beta_o} < b$	$\frac{t_o + y}{1 + \beta_o}$	$\frac{\pi}{2}\sqrt{1 - \beta_o^2} + \frac{\sqrt{t_o^2 - y^2}}{y} + \beta_o \cosh^{-1}\frac{t_o}{y} + \sqrt{1 - \beta_o^2}\sin^{-1}\frac{y - \beta_o t_o}{t_o - \beta_o y}$
8	$\frac{y - t_o}{1 - \beta_o} \leqq 0$	0	$\frac{t_o + y}{1 + \beta_o} \geqq b$	b	$\frac{\sqrt{t_o^2 - y^2}}{y} + \beta_o \cosh^{-1}\frac{t_o}{y} + \sqrt{1 - \beta_o^2}\sin^{-1}\frac{y - \beta_o t_o}{t_o - \beta_o y} - \frac{\sqrt{(t_o - \beta_o b)^2 - (y - b)^2}}{y - b} - \beta_o \cosh^{-1}\frac{t_o - \beta_o b}{y - b} - \sqrt{1 - \beta_o^2}\sin^{-1}\frac{-b(1 - \beta_o^2) + y - \beta_o t_o}{t_o - \beta_o y}$
9	$\frac{y - t_o}{1 - \beta_o} > 0$	$\frac{y - t_o}{1 - \beta_o}$	$\frac{t_o + y}{1 + \beta_o} < b$	$\frac{t_o + y}{1 + \beta_o}$	$\pi\sqrt{1 - \beta_o^2}$
10	$\frac{y - t_o}{1 - \beta_o} > 0$	$\frac{y - t_o}{1 - \beta_o}$	$\frac{t_o + y}{1 + \beta_o} \geqq b$	b	$\frac{\pi}{2}\sqrt{1 - \beta_o^2} - \frac{\sqrt{(t_o - \beta_o b)^2 - (y - b)^2}}{y - b} - \beta_o \cosh^{-1}\frac{t_o - \beta_o b}{y - b} - \sqrt{1 - \beta_o^2}\sin^{-1}\frac{-b(1 - \beta_o^2) + y - \beta_o t_o}{t_o - \beta_o y}$

[1]A table for integral B may be obtained from table I by substituting β_1 for β_o and t_1 for t_o.

TABLE II

INTEGRATION LIMITS OF η AND CORRESPONDING VALUES OF THE INTEGRAL C^1

	Condition	Upper limit	Integral C
$\beta_o > 1$ (The integral exists only when $t_o > y$; the lower limit is always zero.)			
1	$\frac{t_o - y}{1 + \beta_o} < b$	$\frac{t_o - y}{1 + \beta_o}$	$\frac{\sqrt{t_o^2 - y^2}}{y} + \beta_o \cosh^{-1} \frac{t_o}{y} - \sqrt{\beta_o^2 - 1} \cosh^{-1} \left\lvert \frac{-(y + \beta_o t_o)}{t_o + \beta_o y} \right\rvert$
2	$\frac{t_o - y}{1 + \beta_o} \geqq b$	b	$\frac{\sqrt{t_o^2 - y^2}}{y} + \beta_o \cosh^{-1} \frac{t_o}{y} - \sqrt{\beta_o^2 - 1} \cosh^{-1} \left\lvert \frac{-(y + \beta_o t_o)}{t_o + \beta_o y} \right\rvert -$ $\frac{\sqrt{(t_o - \beta_o b)^2 - (y + b)^2}}{y + b} - \beta_o \cosh^{-1} \frac{t_o - \beta_o b}{y + b} - \sqrt{\beta_o^2 - 1} \cosh^{-1} \frac{(\beta_o^2 - 1) b - (y + \beta_o t_o)}{t_o + \beta_o y}$
$\beta_o < 1$ (The integral exists only when $t_o > y$; the lower limit is always zero.)			
	Condition	Upper limit	Integral C
3	$\frac{t_o - y}{1 + \beta_o} < b$	$\frac{t_o - y}{1 + \beta_o}$	$\frac{\pi}{2} \sqrt{1 - \beta_o^2} + \frac{\sqrt{t_o^2 - y^2}}{y} + \beta_o \cosh^{-1} \frac{t_o}{y} - \sqrt{1 - \beta_o^2} \sin^{-1} \frac{y + \beta_o t_o}{t_o + \beta_o y}$
4	$\frac{t_o - y}{1 + \beta_o} \geqq b$	b	$\frac{\sqrt{t_o^2 - y^2}}{y} + \beta_o \cosh^{-1} \frac{t_o}{y} - \sqrt{1 - \beta_o^2} \sin^{-1} \frac{y + \beta_o t_o}{t_o + \beta_o y} -$ $\frac{\sqrt{(t_o - \beta_o b)^2 - (y + b)^2}}{y + b} - \beta_o \cosh^{-1} \frac{t_o - \beta_o b}{y + b} + \sqrt{1 - \beta_o^2} \sin^{-1} \frac{b(1 - \beta_o^2) - (y + \beta_o t_o)}{t_o + \beta_o y}$

[1]A table for integral D may be obtained from table II by substituting β_1 for β_o and t_1 for t_o.

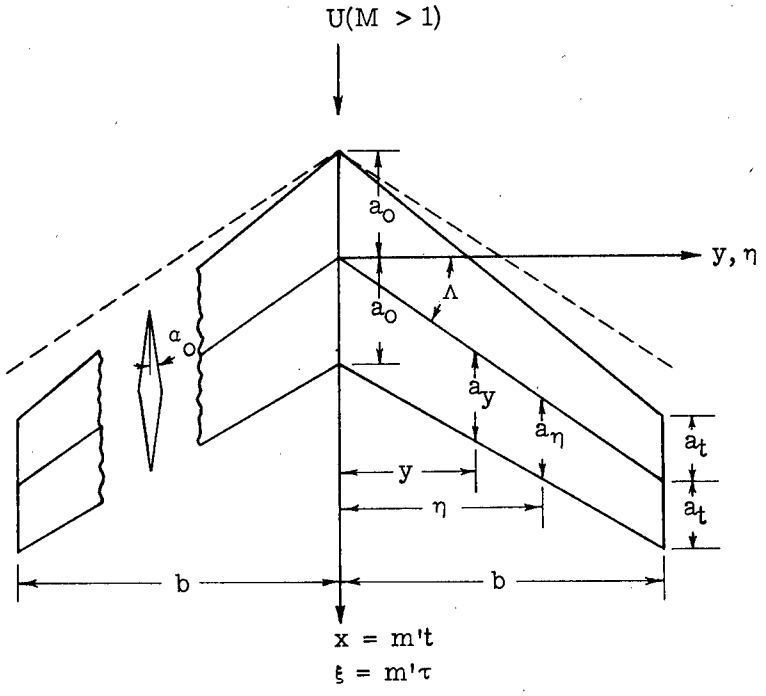

(a) In physical plane (x,y).

Figure 1.- Sweptback wing in physical and transformed planes.

PARAMETER RELATIONS BETWEEN PHYSICAL PLANE (x,y) AND TRANSFORMED PLANE (t,y)

a_o half root chord	$a_o' = a_o/m'$
a_t half tip chord	$a_t' = a_t/m'$
b half span	$b' = \frac{b}{a_o'} = \frac{1+\sigma}{2\beta}$ A tan Λ
tan Λ	$\beta = \frac{\tan \Lambda}{m'}$
$\nu = \frac{a_o - a_t}{b}$	$\nu' = \frac{\nu}{m'} = \frac{1-\sigma}{b'} = \frac{2\beta}{A \tan \Lambda} \frac{1-\sigma}{1+\sigma}$
$a_y = a_o - \nu\lvert y\rvert$	$a' = a_y/m'$
$\sigma = a_t/a_o$	$\sigma = 1 - \nu' b'$
$A = \frac{2b}{a_o + a_t}$	$A = \frac{2b'}{m'(1+\sigma)}$
$m' = \sqrt{M^2 - 1}$	$\beta_1 = \beta - \nu'$
α_o surface slope	$\beta_o = \beta + \nu'$

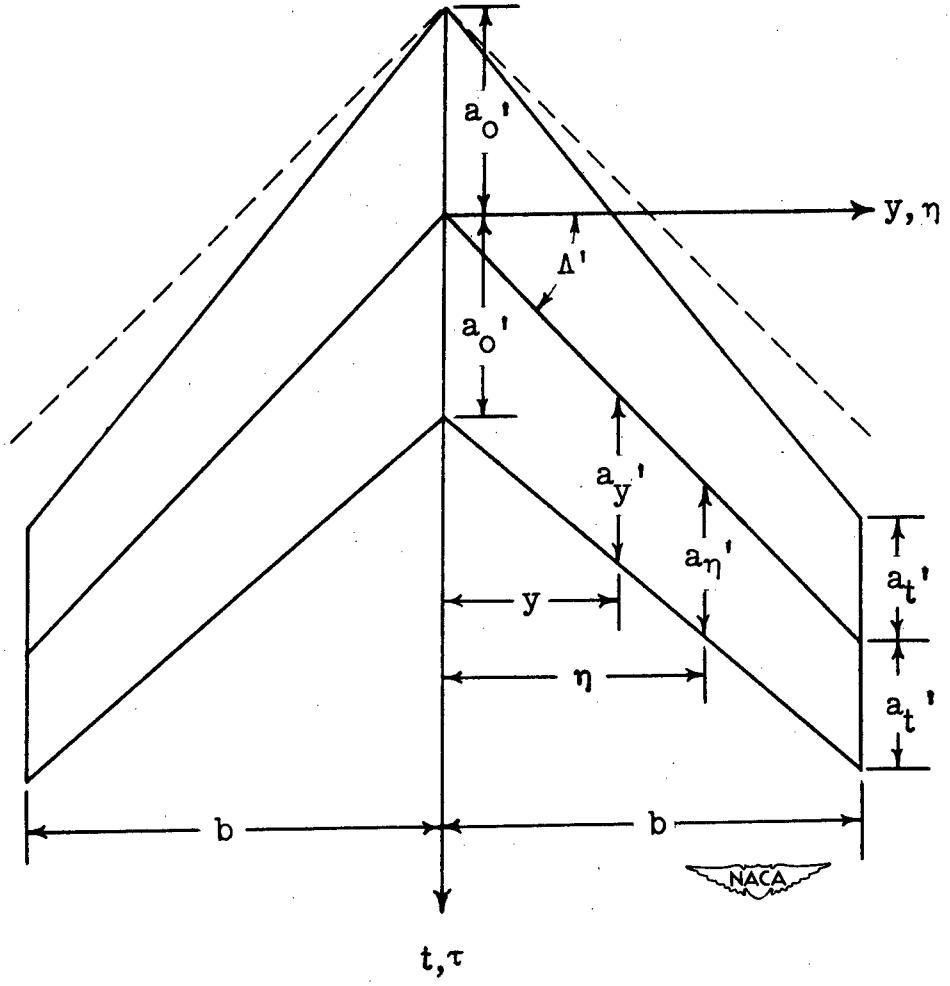

(b) In transformed plane (t,y). Mach line at 45°.

Figure 1.- Concluded.

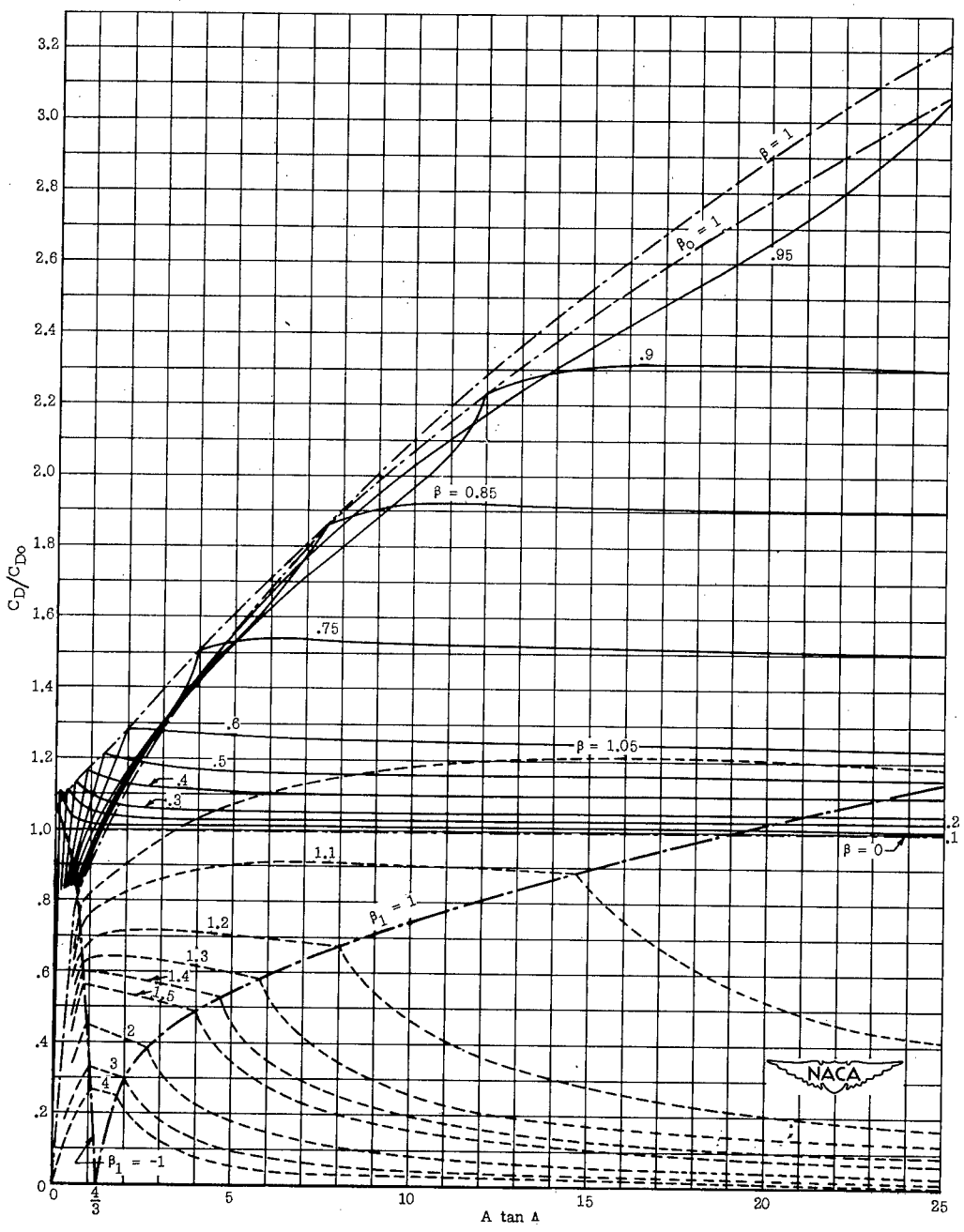

Figure 2.- Wave drag coefficients for the family of sweptback wings with taper ratio of 0.2.

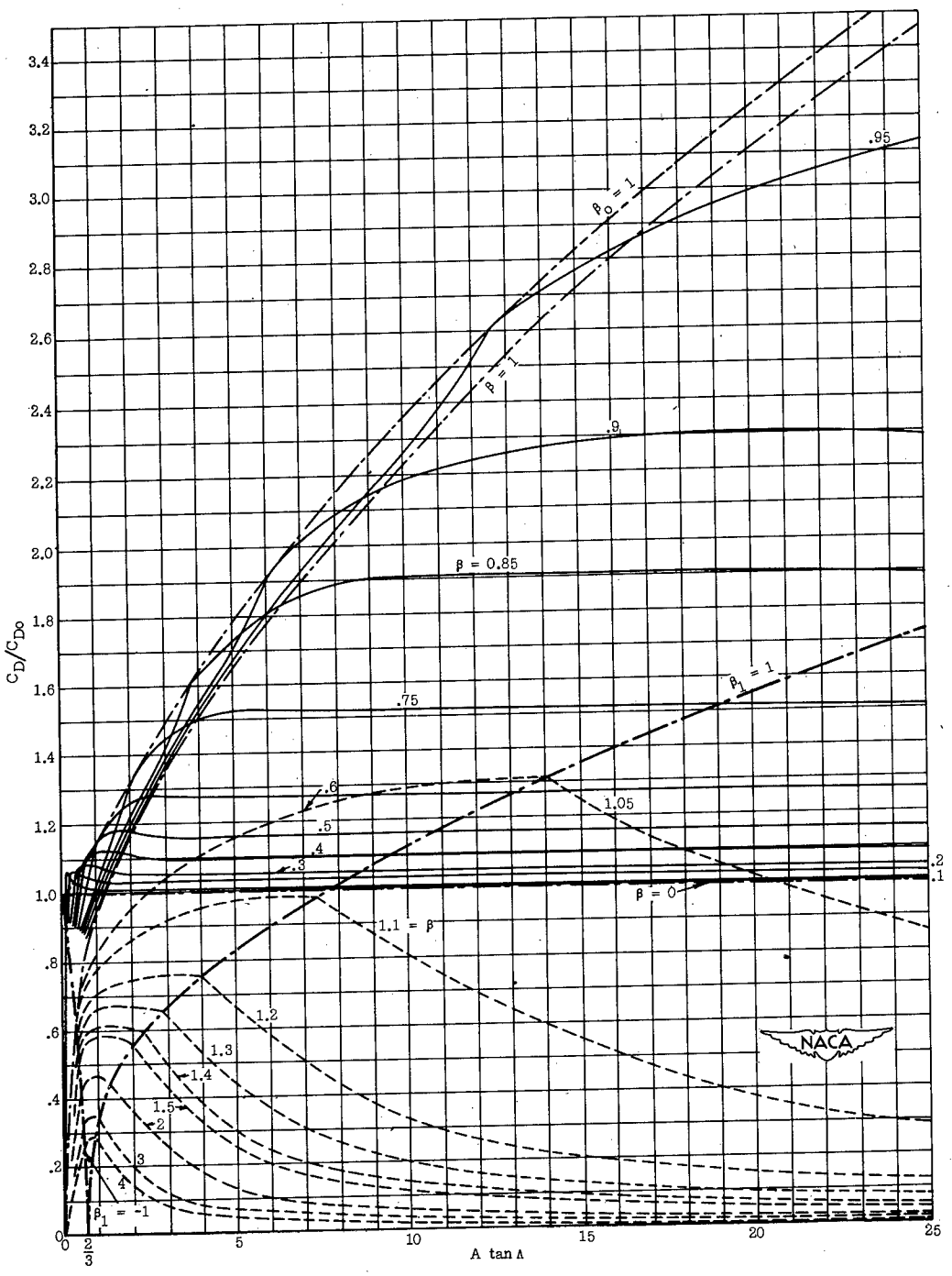

Figure 3.- Wave drag coefficients for the family of sweptback wings with taper ratio of 0.5.

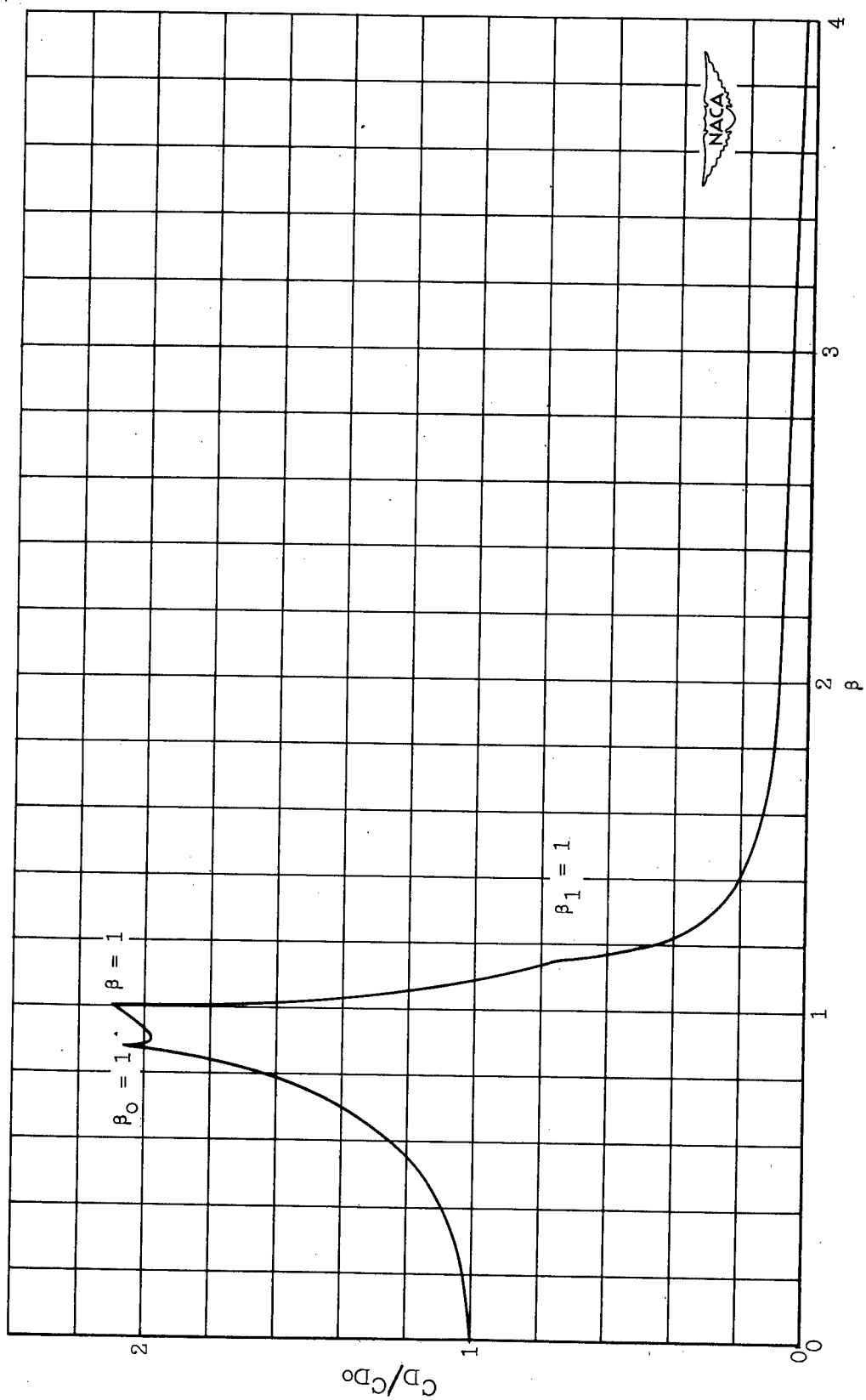

Figure 4.- Plot of C_D/C_{Do} against β for a family of sweptback wings with A tan Λ = 10 and σ = 0.2.

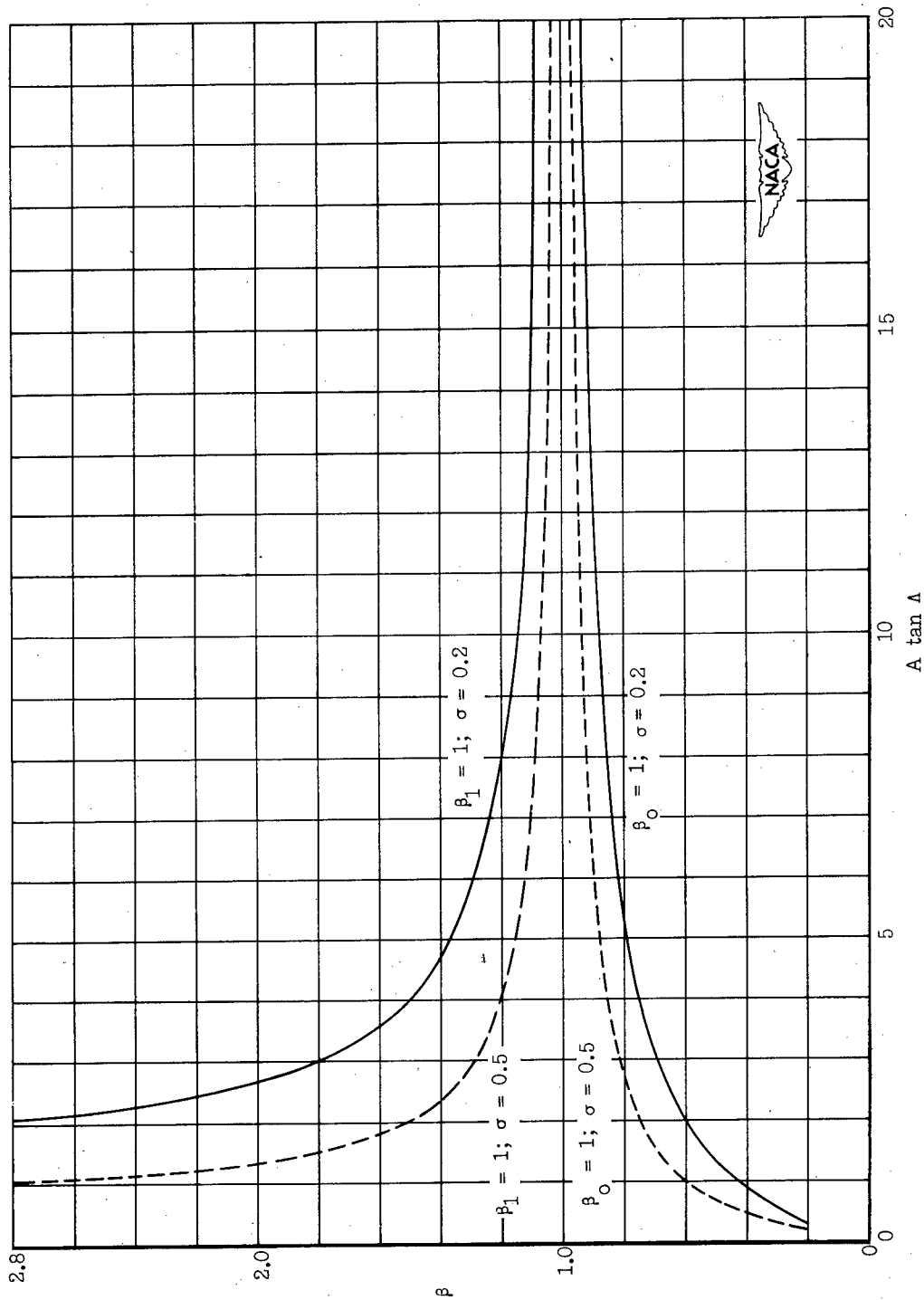

Figure 5.- Location of cusps ($\beta_o = 1$ and $\beta_1 = 1$) of the wave drag parameter C_D/C_{Do} in terms of β and A tan Λ at $\sigma = 0.2$ and 0.5.

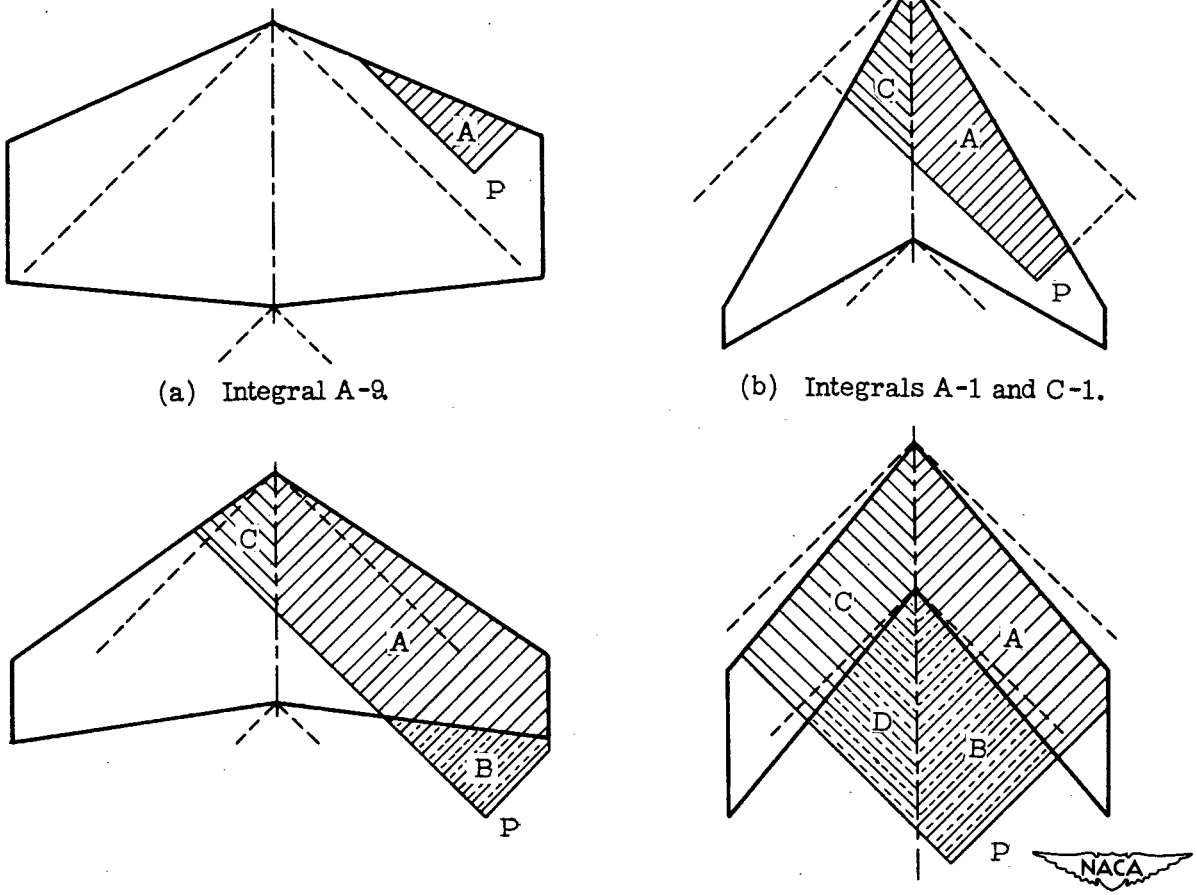

(a) Integral A-9.

(b) Integrals A-1 and C-1.

(c) Integrals A-8, B-10, and C-3.

(d) Integrals A-2, B-1, C-1, and D-1.

Figure 6.- Four typical cases concerning integrals. See tables for identifying letters and numbers.

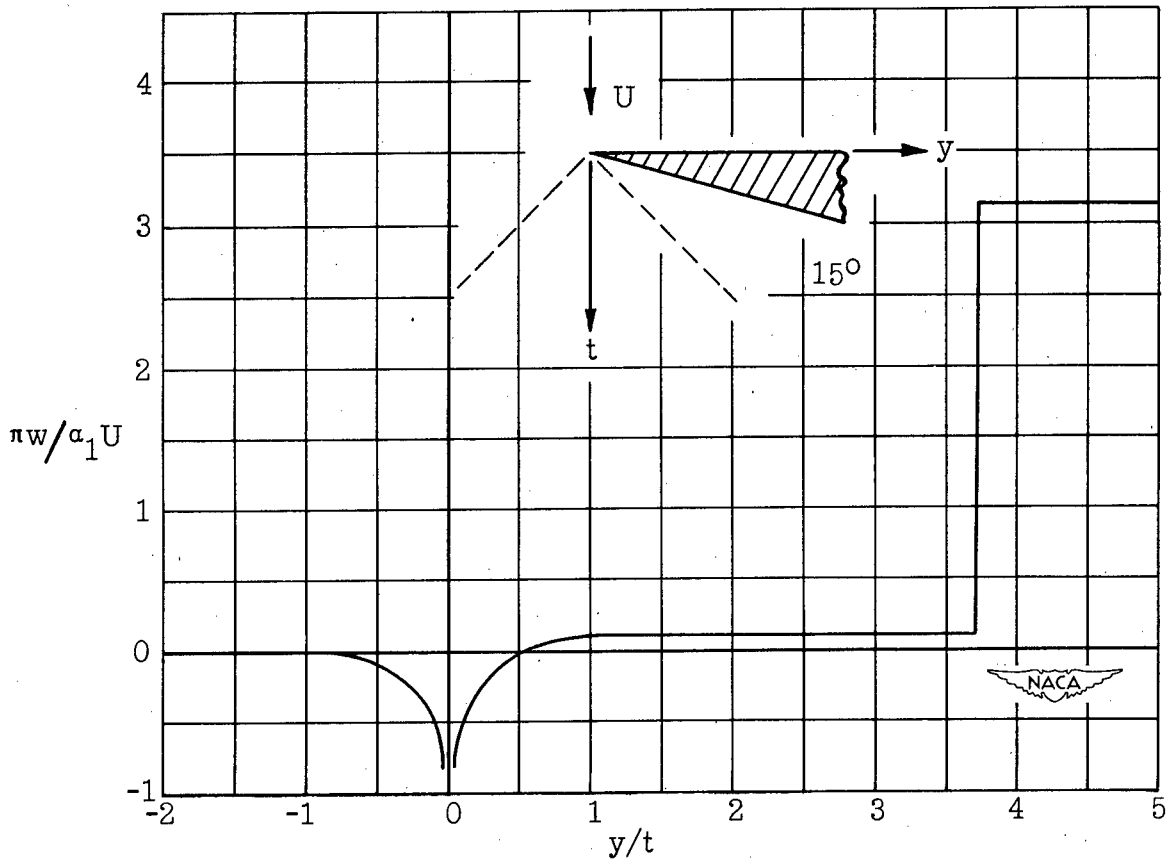

(a) Trailing edge at 15° from leading edge which is normal to direction of flight.

Figure 7.- Downwash distribution for three infinite half-wings.

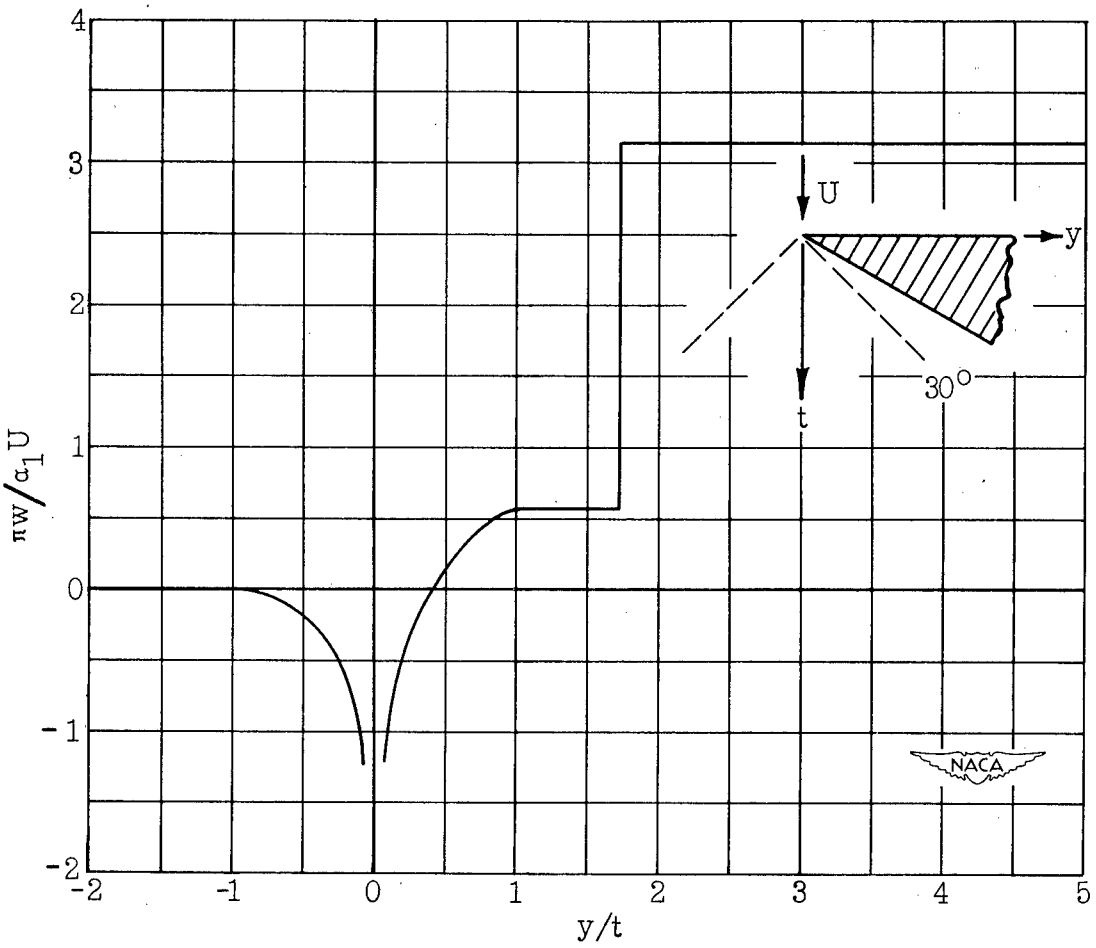

(b) Trailing edge at 30° from leading edge which is normal to direction of flight.

Figure 7.- Continued.

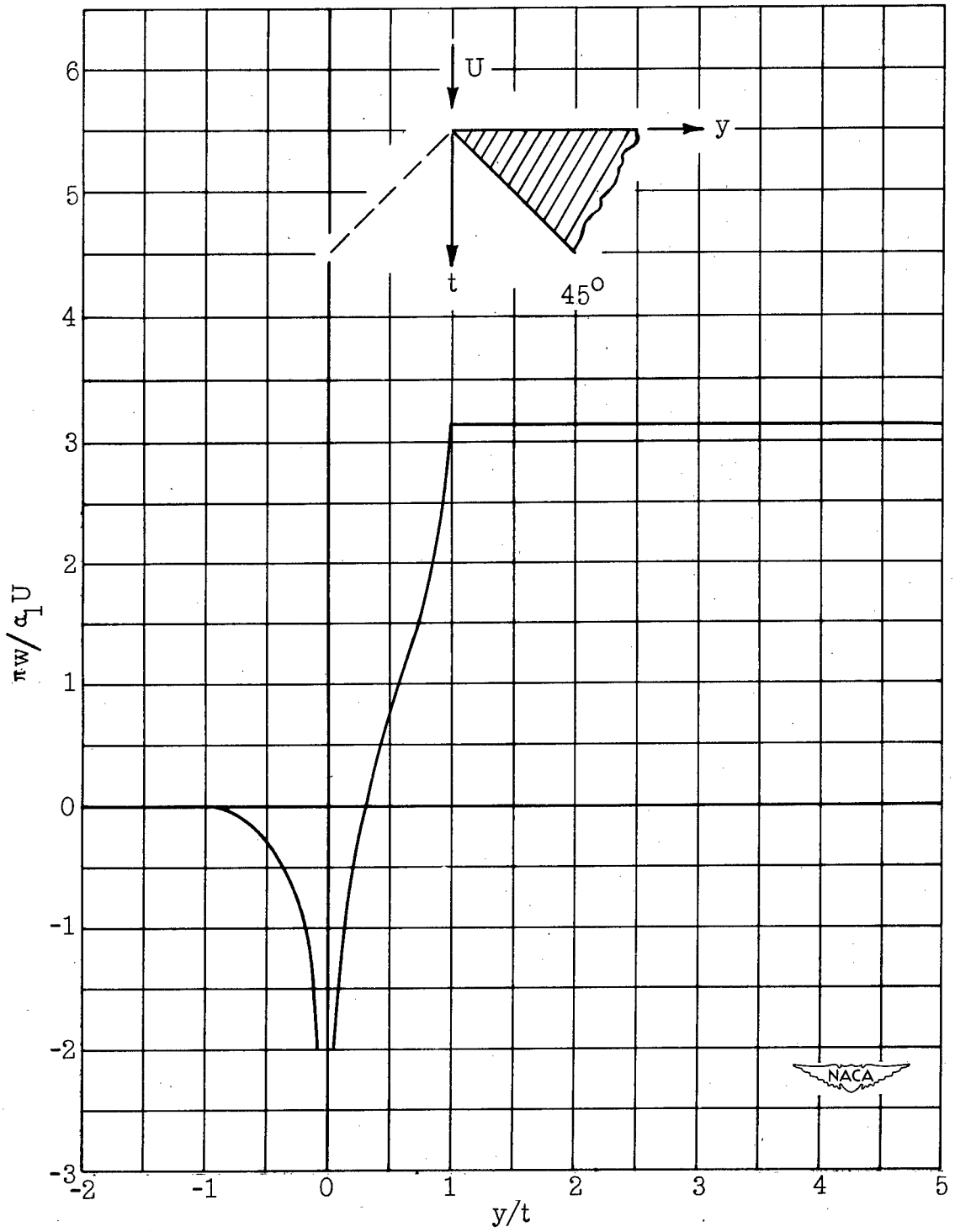

(c) Trailing edge at 45° from leading edge which is normal to direction of flight.

Figure 7.- Concluded.

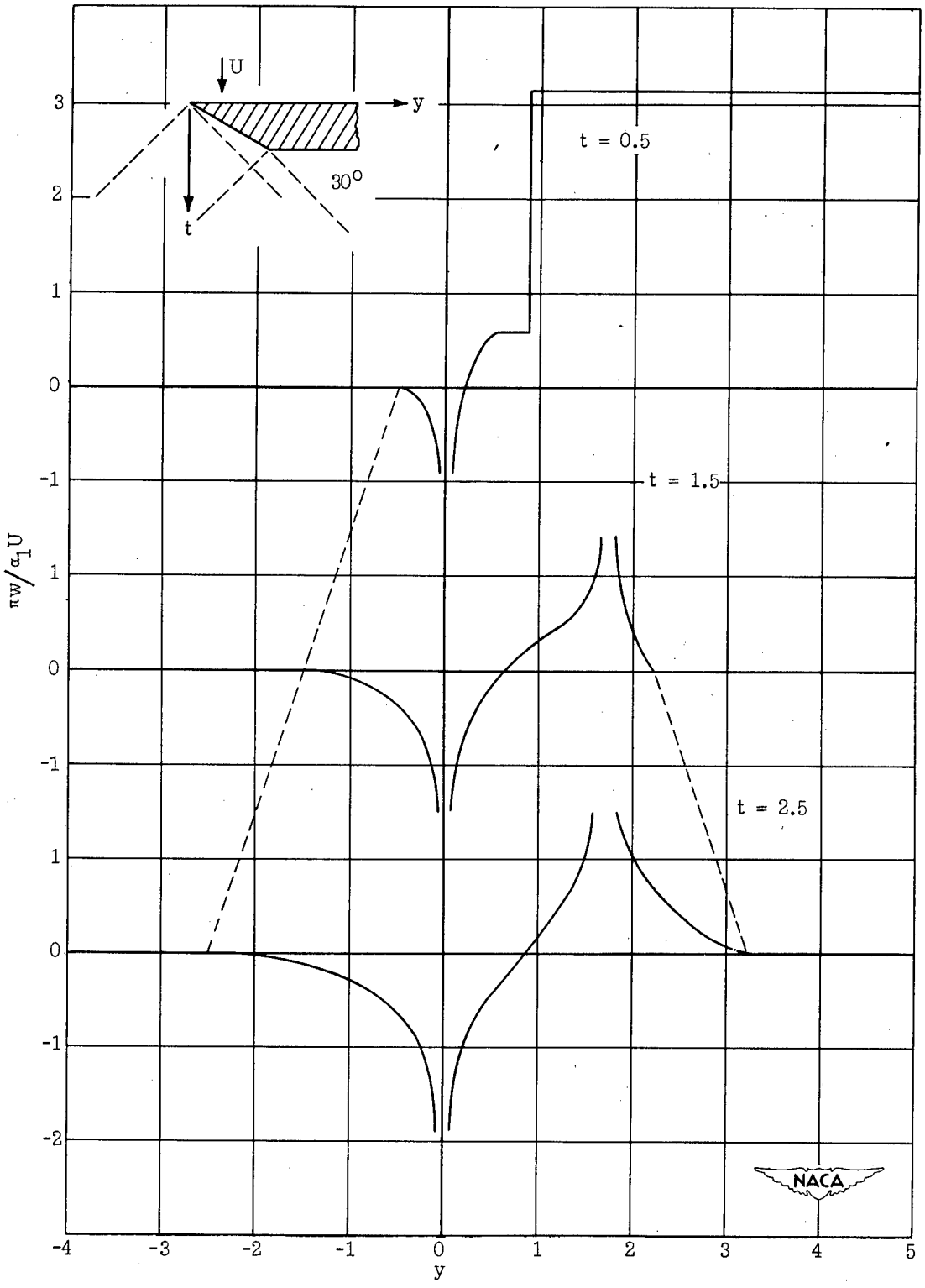

Figure 8.- Downwash distribution over a wing tip of unit chord with a raked angle of 30° for three values of t.

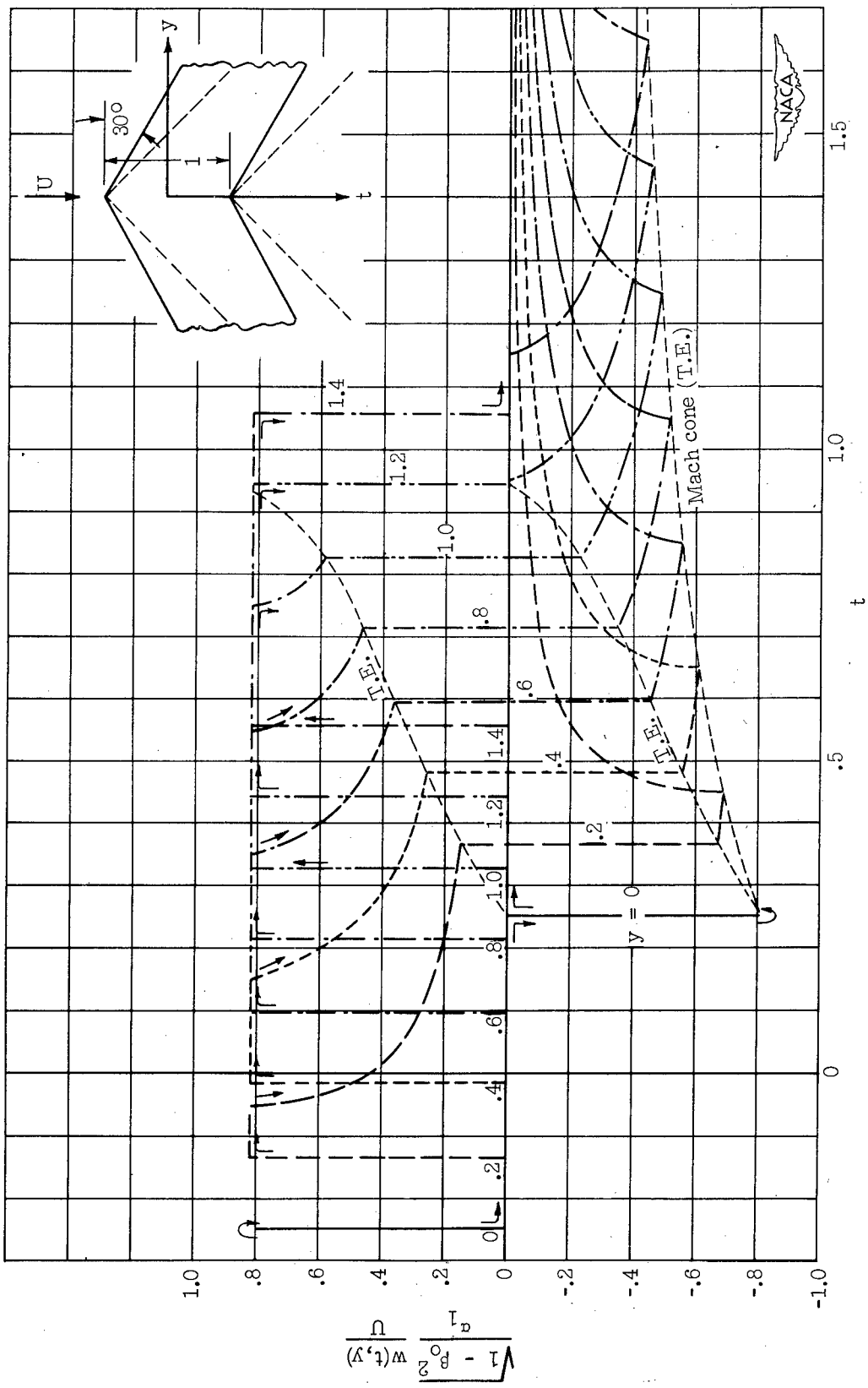

Figure 9.- Downwash distribution near the nose of an infinite constant-chord sweptback wing.

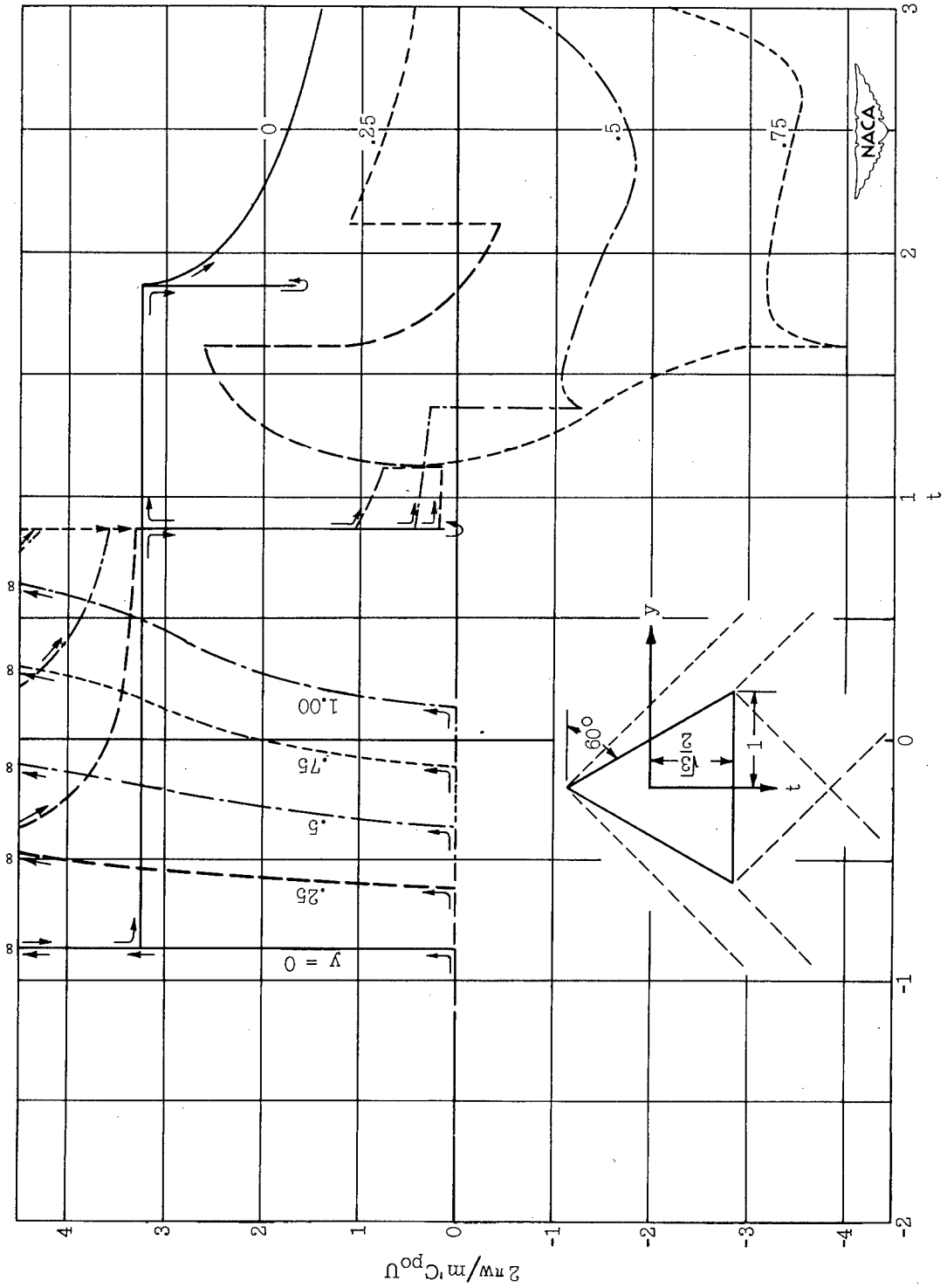

Figure 10.- Downwash distribution at different values of y of a finite triangular wing with a 60° sweptback angle.

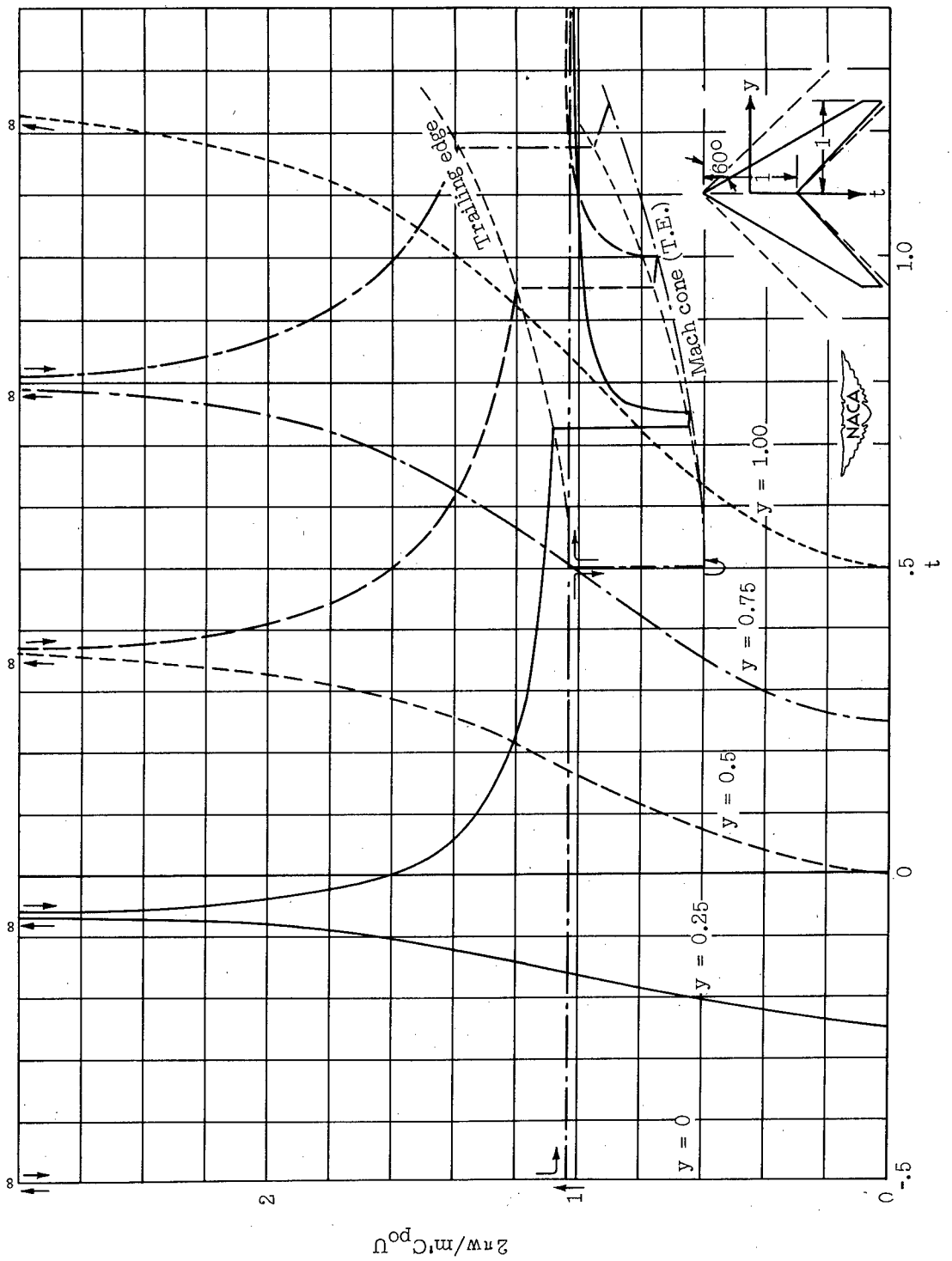

Figure 11.- Downwash distribution at different values of y of a tapered sweptback wing. $\sigma = 1/6$.

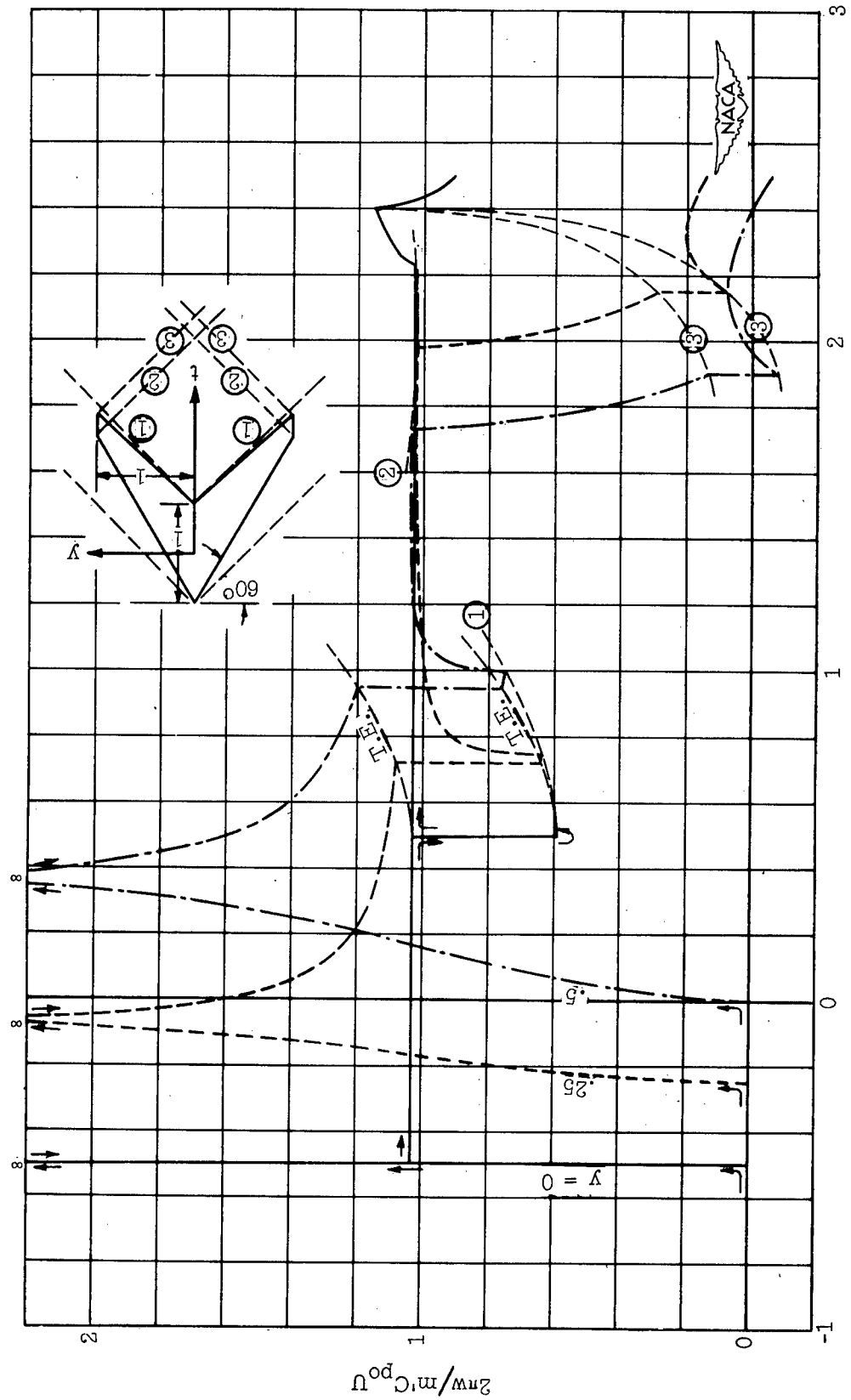

Figure 12.- Downwash distribution at different values of y of a tapered sweptback wing far downstream.